

# Industrial Chemistry & Materials

Online ISSN 2755-2500

Print ISSN 2755-2608

Volume 1 Number 4

November 2023

rsc.li/icm

Themed issue  
Frontiers of Hydrogen Energy and Fuel Cell



## REVIEW ARTICLE

Leiduan Hao, Zhenyu Sun *et al.*

Lithium-mediated electrochemical dinitrogen reduction reaction



ROYAL SOCIETY  
OF CHEMISTRY





Cite this: *Ind. Chem. Mater.*, 2023, 1, 563

## Lithium-mediated electrochemical dinitrogen reduction reaction

Muhammad Saqlain Iqbal,<sup>†b</sup> Yukun Ruan,<sup>†a</sup> Ramsha Iftikhar,<sup>iD</sup> <sup>c</sup> Faiza Zahid Khan,<sup>d</sup> Weixiang Li,<sup>a</sup> Leiduan Hao,<sup>\*a</sup> Alex W. Robertson,<sup>iD</sup> <sup>e</sup> Gianluca Percoco<sup>f</sup> and Zhenyu Sun<sup>iD</sup> <sup>\*a</sup>

The Haber–Bosch process is the dominant approach for NH<sub>3</sub> production today, but the process has to be maintained at energy-intensive high temperatures and pressures. Li-mediated electrocatalytic dinitrogen reduction reaction (eN<sub>2</sub>RR) could instead enable sustainable and green NH<sub>3</sub> production at ambient conditions. Lithium mediators realize the synthesis of NH<sub>3</sub> via the formation of Li<sub>3</sub>N, and thus lower the energy required for the direct cleavage of N<sub>2</sub>. There has now been a surge of interest in devising approaches to optimize the NH<sub>3</sub> yield rate and faradaic efficiency of the eN<sub>2</sub>RR process by employing different catalysts as well as electrolytes. This review discusses the recent advances in the field of the Li-mediated eN<sub>2</sub>RR along with the latest insights into the proposed catalytic mechanisms. Moreover, it also highlights the state-of-the-art reported electrocatalysts and electrolytes that have revolutionized the field of the Li-mediated eN<sub>2</sub>RR. In addition to the above, our review provides a critical overview of certain limitations and a future prospectus that will provide a way forward to explore this area.

Received 15th January 2023,  
Accepted 3rd April 2023

DOI: 10.1039/d3im00006k

rs.c.li/icm

Keywords: Nitrogen reduction reaction; Ammonia; Electrocatalysis; Lithium; Reaction mechanism.

### 1 Introduction

Ammonia (NH<sub>3</sub>) is a crucial chemical fertilizer for crop development that has supported the rapid increase in our global population. It has high hydrogen content, a large gravimetric energy density comparable to methanol, and is easy to liquefy for storage and transit, among other beneficial properties. The global production of NH<sub>3</sub> is expected to increase to about 290 million tons by 2030. In 2022, the global ammonia market was valued at USD 78.26 billion and is expected to reach USD 129.63 billion by 2030, with a projected compound annual growth rate (CAGR) of 6.51% during the forecast period from 2022 to 2030 (Fig. 1).<sup>2</sup> Table 1 provides an overview of the global NH<sub>3</sub> market from

2021 to 2030, including the market size in 2022 and the projected market size by 2030, with a forecasted CAGR of 6.51% from 2022 to 2030. The report studied different global regions, and found that the Asia-Pacific region is the largest market for ammonia products, followed by North America. The report also accounted for different segments of the ammonia market, including the product form and application.<sup>2</sup> The large-scale centralized Haber–Bosch (HB) process is the current favored industrial technique for realizing this sizeable international demand and delivering the mass production of NH<sub>3</sub>. In the HB process N<sub>2</sub> reacts with H<sub>2</sub> (N<sub>2</sub> + 3H<sub>2</sub> → 2NH<sub>3</sub>) on an Fe-based catalyst, and is typically operated at high temperatures (400–500 °C) and high pressure (150–250 bar), resulting in high energy use and cost.<sup>1</sup> Due to the combination of high and growing demand for NH<sub>3</sub>, and the high temperature requirements of the HB process, it is urgent to develop new catalysts and procedures for NH<sub>3</sub> synthesis that can reduce the energy required and the carbon footprint.

In order to find alternatives to the energy-intensive H–B process, scientists have searched for catalysts that might avoid the direct cleavage of the dinitrogen triple bond and that can produce NH<sub>3</sub> when powered by electricity.<sup>3,4</sup> The reduction of dinitrogen (N<sub>2</sub>) by electrocatalysis has been studied extensively over the past few years using a variety of electrocatalysts. However, it has been revealed that even the best reported catalysts could only use 1% of the electrons to

<sup>a</sup> State Key Laboratory of Organic–Inorganic Composites, College of Chemical Engineering, Beijing University of Chemical Technology, Beijing 100029, P. R. China. E-mail: haold@buct.edu.cn, sunzy@mail.buct.edu.cn

<sup>b</sup> Department of Electrical and Information Engineering, Polytechnic University of Bari, Via E. Orabona 4, 70125 Bari, Italy

<sup>c</sup> School of Chemistry, University of New South Wales, 2033 Sydney, Australia

<sup>d</sup> Institute of Chemistry, Rheinische Friedrich-Wilhelms-Universität Bonn, 53113 Bonn, Germany

<sup>e</sup> Department of Physics, University of Warwick, Coventry CV4 7AL, UK

<sup>f</sup> Department of Mechanics, Mathematics and Management, Polytechnic University of Bari, Via E. Orabona 4, 70125 Bari, Italy

<sup>†</sup> These authors contributed equally to this work.



produce  $\text{NH}_3$  in aqueous solutions because of the competitive hydrogen evolution reaction (HER). Recently, the lithium-mediated  $\text{N}_2$  reduction reaction (Li-e $\text{N}_2$ RR) has been found to be a promising route for electrochemical  $\text{NH}_3$  synthesis at ambient conditions. The Li-e $\text{N}_2$ RR was first attempted in an alcoholic solution of lithium halide in 1930 by Fichter and coworkers.<sup>5</sup> Tsuneto *et al.* further improved the faradaic efficiency (FE) by employing an electrolyte with tetrahydrofuran (THF) mixed with ethanol (EtOH) and increasing the  $\text{N}_2$  pressure.<sup>6</sup> Lee *et al.*<sup>7</sup> reported that lithium used along with the electrolyte solution acted as a mediator, as the  $\text{Li}^+$  ions after reduction allow for the conversion of  $\text{N}_2$  gas into  $\text{Li}_3\text{N}$ . Moreover, this Li-mediated system can be modified with superhydrophobic metal organic frameworks (MOFs) to suppress the competing HER and enhance the e $\text{N}_2$ -

RR. The greatest advantage of Li-e $\text{N}_2$ RR is that the active Li and inert proton source can promote  $\text{N}_2$  activation and hinder  $\text{H}_2$  evolution, respectively. However, a majority of Li-e $\text{N}_2$ RR studies have the limitation of using a sacrificial solvent as a proton donor, prohibiting the scale up synthesis in batch cells.

## 2 Li-mediated e $\text{N}_2$ RR

For  $\text{NH}_3$  synthesis, a wide range of different catalytic materials and systems have been investigated. It has been suggested that Li in particular holds the potential of producing  $\text{NH}_3$  at ambient pressure. The rate-determining step in the synthesis of  $\text{NH}_3$  is often the adsorption and activation of  $\text{N}_2$ .<sup>8–14</sup> Li has an extraordinarily low work



**Muhammad Saqlain Iqbal**

*Muhammad Saqlain Iqbal has earned his Master's degree from COMSATs University Islamabad (2021) and is currently pursuing his Ph.D. from Politecnico di Bari. He is working under the supervision of the distinguished Professor Gianluca Percoco, a renowned expert in the field of materials science and engineering. Mr. Iqbal has a keen interest in the development of 3D printed batteries, with a particular focus on lithium and solid-state batteries. His research is motivated to improve energy storage, he explores innovative techniques and materials to enhance battery performance, including energy density, power density, and cycle life while ensuring efficiency, affordability, and sustainability.*



**Yukun Ruan**

*Yukun Ruan received his BS degree in Beijing University of Chemical Technology in 2020. He is pursuing his MS degree in Beijing University of Chemical Technology under the supervision of Prof. Zhenyu Sun. His current research interest is  $\text{N}_2$  reduction reaction.*



**Leiduan Hao**

*Dr. Leiduan Hao received her PhD in materials science at Institute of Chemistry, Chinese Academy of Sciences in 2016. From 2017 to 2021, she worked at Washington State University as a postdoctoral research associate to study the design of novel porous materials for green catalysis. Then she joined the Sun group at Beijing University of Chemical Technology (China) as an associate professor. Currently, her research mainly focuses on  $\text{CO}_2$  and  $\text{N}_2$  conversion.*



**Zhenyu Sun**

*Zhenyu Sun completed his PhD at the Institute of Chemistry Chinese Academy of Sciences in 2006. He carried out postdoctoral research at Trinity College Dublin (Ireland, 2006–2008), Ruhr University, Bochum (Germany, 2011–2014), and the University of Oxford (UK, 2014–2015). He is currently a full professor at the College of Chemical Engineering at Beijing University of Chemical Technology (China). He was awarded a Humboldt Research Fellowship for Experienced Researchers (Germany). His current research focuses on energy conversion reactions including  $\text{N}_2$  reduction reaction and  $\text{CO}_2$  reduction reaction.*



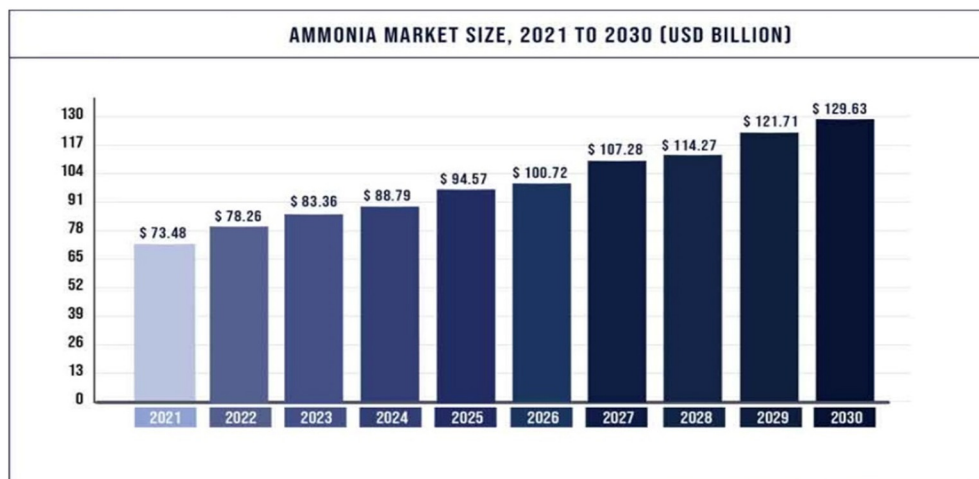


Fig. 1 Projected global ammonia demand growth from 2021 to 2030.<sup>2</sup> Copyright 2023, Precedence Research.

Table 1 Overview of global ammonia market (2021–2030)<sup>2</sup>

| Report coverage               | Detail                                                                                                                                                                   |
|-------------------------------|--------------------------------------------------------------------------------------------------------------------------------------------------------------------------|
| Market size in 2022           | USD 78.26 billion                                                                                                                                                        |
| Market size by 2030           | USD 129.63 billion                                                                                                                                                       |
| Growth rate from 2022 to 2030 | CAGR of 6.51%                                                                                                                                                            |
| Largest market                | Asia-Pacific                                                                                                                                                             |
| Second largest market         | North America                                                                                                                                                            |
| Base year                     | 2021                                                                                                                                                                     |
| Forecast period               | 2022 to 2030                                                                                                                                                             |
| Segments covered              | <ul style="list-style-type: none"> <li>• By product form</li> <li>• By application</li> </ul>                                                                            |
| Regions covered               | <ul style="list-style-type: none"> <li>• North America</li> <li>• Europe</li> <li>• Asia-Pacific</li> <li>• Latin America</li> <li>• Middle East &amp; Africa</li> </ul> |

function and high reactivity for this process. Li can therefore be used to break the strong N≡N triple bond and fix N<sub>2</sub> as Li<sub>3</sub>N, which subsequently converts to NH<sub>3</sub>. Additionally, Li<sup>+</sup> ions have been shown to disrupt the water molecule, which lowers the rate of water splitting.<sup>15</sup> According to the study by McEnaney *et al.*, Li may undergo electro-cycling to create NH<sub>3</sub> in a molten electrolyte at atmospheric pressure with an extremely high NH<sub>3</sub> FE of 88.5%.<sup>1</sup> A larger applied energy (potential) is required for the electrodeposition of Li at the cathode, which stabilizes N<sub>2</sub> in the form of Li<sub>3</sub>N. This study further demonstrated that Li<sup>0</sup> can facilitate the electrochemical reduction of N<sub>2</sub> to NH<sub>3</sub>. An NH<sub>3</sub> FE of 57.7% was attained with an Fe electrode using 0.2 M LiClO<sub>4</sub> in THF as the electrolyte and 0.18 M ethanol as the proton source while operating under high pressure (50 atm) of N<sub>2</sub>.<sup>6</sup> Li<sup>+</sup> ions were found to inhibit the competitive HER on the surface of Pt while promoting the HER on Au.<sup>16</sup> As opposed to this study, Suo *et al.* instead attributed the suppression of the HER to the decomposition of the TFSI anion in the formed lithium bis(trifluoromethane sulfonyl) imide (LiTFSI) salt. Due to the electrodes' weak selectivity for N<sub>2</sub> reduction,

ambient eN<sub>2</sub>RR in an aqueous electrolyte remains a difficult task.<sup>17,18</sup> Since the standard potential needed for the eN<sub>2</sub>RR is close to that of the HER, the N<sub>2</sub> reduction reaction in aqueous electrolytes is usually accompanied by the HER.<sup>19</sup> Therefore, approaches that either hamper the HER by changing to an electrocatalyst with weak H<sup>+</sup> adsorption, or by changing the electrolyte (for instance, to non-aqueous systems) are required to be developed.<sup>20</sup>

The Li-mediated eN<sub>2</sub>RR for NH<sub>3</sub> synthesis driven by renewably generated electricity has garnered a lot of recent scientific interest.<sup>21–23</sup> Due to competition with HER and the high stability of the N≡N triple bond, the key challenge is to significantly improve efficiency and the rate of NH<sub>3</sub> generation. Ethanol is frequently applied as the local proton source, which however may deteriorate in the reaction environment. In a THF solution containing 1% ethanol, Lazouski *et al.* attained an NH<sub>3</sub> production rate of 7.9 × 10<sup>-9</sup> mol cm<sup>-2</sup> s<sup>-1</sup> and a maximum NH<sub>3</sub> FE of 18.5% via the Li-mediated eN<sub>2</sub>RR.<sup>11</sup> A more encouraging result was achieved in a phosphonium salt in place of ethanol, with an NH<sub>3</sub> production rate approaching approximately 6.0 × 10<sup>-8</sup> mol cm<sup>-2</sup> s<sup>-1</sup> and an NH<sub>3</sub> FE of roughly 69% for 20 h under 0.05 MPa H<sub>2</sub> and 1.95 MPa N<sub>2</sub>.<sup>24</sup>

In order to alleviate the unwanted HER and achieve an initial current efficiency of 88.5%, electrochemical lithium cycling was proposed as an effective method for manufacturing NH<sub>3</sub>, which requires independent steps of LiOH electrolysis, direct nitridation of Li, and release of NH<sub>3</sub> from Li<sub>3</sub>N. However, this multi-step process is difficult to operate, and the step that involves LiOH electrolysis for Li regeneration is particularly challenging. Jain *et al.* synthesized NH<sub>3</sub> through hydrolysis of Li<sub>3</sub>N at 80 °C in a closed cycle and Li-metal was reproduced at the end of the reaction.<sup>25</sup> In addition to using Li-Sn alloys for breaking the N≡N triple bond to produce Li<sub>3</sub>N, which was subsequently used for NH<sub>3</sub> synthesis below 500 °C under 0.5 MPa, Yamaguchi *et al.* also reported the use of pure Li to fix N<sub>2</sub>. The same research group has recently established a three-



step pseudo-catalytic method for the production of  $\text{NH}_3$  below 400 °C under 0.1 MPa by reacting solid Li–Sn alloy with  $\text{N}_2$  and  $\text{H}_2$  consecutively, followed by regeneration of the initial alloy in a chemical loop. The maximum molar proportion of  $\text{NH}_3$  is equivalent to one-tenth of the composition at thermodynamic equilibrium. The Li–Sn catalyst system's stability, however, was not the subject of a thorough study. Since the solid Li–Sn alloy, as well as the produced  $\text{Li}_3\text{N}$  and  $\text{LiH}$ , are sensitive to  $\text{O}_2$  and  $\text{H}_2\text{O}$ , its deactivation is a significant problem.<sup>26</sup> Additionally, the scaling relationship between the activation barrier for  $\text{N}_2$  dissociation and the  $\text{N}_2$ -binding energy limits Li, much like it does for transition metals (TMs). In  $\text{Li}_3\text{N}$ , nitrogen is strongly bound to lithium.  $\text{Li}_3\text{N}$  can react with  $\text{H}_2$  to produce a mixture of  $\text{LiNH}_2$ ,  $\text{Li}_2\text{NH}$ , and  $\text{LiH}$  at relatively low temperatures, but it is difficult to further hydrogenate  $\text{LiNH}_2$  and  $\text{Li}_2\text{NH}$  to produce  $\text{LiH}$  and  $\text{NH}_3$  for both thermodynamic and kinetic reasons.

The question of how to overcome Li's scaling relation is an enormous challenge but has been rarely studied. One method discussed by McEnaney calls for separate  $\text{N}_2$  fixation stages in the absence of a proton source and the subsequent exothermic release of  $\text{NH}_3$  by exposing the solid  $\text{Li}_3\text{N}$  to  $\text{H}_2\text{O}$  rather than  $\text{H}_2$ .<sup>1</sup> While TMs offer insights into catalyst design, further work has been reported on circumventing the scaling relation imposed on TMs. For instance, introducing alkali metals or oxides as promoters resulted in an increased  $\text{NH}_3$  synthesis rate and mitigated the well-known pure-TM scaling relation by creating local electrical fields.<sup>27,28</sup> Wang *et al.* also found that employing  $\text{LiH}$  to mediate  $\text{N}_2$  transfer and  $\text{NH}_3$  production broke the scaling relation on TMs. Instead of using Li's high activity to fix  $\text{N}_2$ ,  $\text{LiH}$ 's negatively charged hydrogen ions can serve as potent reducing agents when reacting with  $\text{N}_2$  atoms that have been activated by the right solid-state transition metal to create  $\text{LiNH}_2$ . Then,  $\text{H}_2$  and  $\text{LiNH}_2$  interact to form  $\text{NH}_3$  and regenerate  $\text{LiH}$ . The  $\text{LiH}$  and TM work together to overcome the scaling relation on TMs and enable an energy-efficient  $\text{NH}_3$  production.<sup>29</sup> Additionally,  $\text{NH}_3$  synthesis was demonstrated to be mediated by alkali or alkaline earth metal hydride/imide pairings (*e.g.*,  $\text{LiH}/\text{Li}_2\text{NH}$ ,  $\text{BaH}_2/\text{BaNH}$ ) with an ability to disrupt the scaling relation comparable to Fe, Co, and Ni in the  $\text{N}_2$  fixation stage.<sup>30</sup>

The most commonly used aqueous electrolytes in  $\text{NH}_3$  synthesis include alkaline electrolytes ( $\text{KOH}$  and  $\text{KHCO}_3$ ),<sup>31,32</sup> acidic electrolytes ( $\text{HCl}$  and  $\text{H}_2\text{SO}_4$ ), and  $\text{LiClO}_4$ - and  $\text{Li}_2\text{SO}_4$ -based neutral electrolytes.<sup>3,33</sup> These Li-mediated aqueous electrolytes have been identified as promising potential electrolytes due to the improved interaction between  $\text{Li}^+$  and  $\text{N}_2$ .<sup>34,35</sup> Because large cations include core electrons, the stabilizing impact of the electrostatic and induction effects on the total energy is constrained, leading to the conclusion that  $\text{Li}^+$  is more effective than  $\text{Na}^+$  for  $\text{N}_2$  adsorption.<sup>36</sup> An order of  $\text{Ca}^{2+} > \text{Na}^+ > \text{Li}^+$  was proposed, in which the adsorption energies for  $\text{N}_2$  decrease.<sup>35</sup> Chen *et al.* recently employed the  $\text{Li}^+$  incorporation approach, which not only

resulted in slow kinetics and a higher energy barrier for the generation of  $\text{H}_2$ , but also provided suitable  $\text{eN}_2\text{RR}$  sites.  $\text{LiClO}_4$  has been demonstrated to deliver better  $\text{NH}_3$  FE and yield rate compared to  $\text{NaClO}_4$  and  $\text{KClO}_4$  electrolytes because of the improved interactions between  $\text{Li}^+$  and  $\text{N}_2$ .<sup>32</sup>

The performance of  $\text{eN}_2\text{RR}$  is dependent on the electrolysis current and the freshness of lithium deposits. A higher current results in fresher lithium deposits, which exposes more active lithium to nitrogen and enhances  $\text{eN}_2\text{-RR}$ . In contrast, a low current leads to passivation of lithium, deteriorating its reactivity towards  $\text{eN}_2\text{RR}$ . Strategies such as retarding passivation or creating a protective layer may be employed to improve  $\text{N}_2\text{RR}$  efficiency. One approach is to use electrolyte additives to engineer the solid-electrolyte interphase to create a protective layer that is impervious to electrolyte but penetrable by nitrogen and proton source.<sup>37</sup>

Although there are still obstacles to the practical viability of lithium-mediated ammonia synthesis, such as the need for a replacement for the sacrificial proton source, a promising alternative to  $\text{N}_2$  pressure for independently increasing the mass transport of  $\text{N}_2$  relative to protons could be the use of gas diffusion electrodes. According to the model by Andersen,<sup>38</sup> a higher rate at a similar FE could be achieved if the transfer rate of  $\text{N}_2$  to the surface were to be increased proportionally. This model highlights the unique features of the lithium-mediated process. Lithium has a strong binding affinity for nitrogen and a low barrier for  $\text{N}_2$  dissociation,<sup>1</sup> similar to early transition metals and nitrides.<sup>19,39</sup> However, only lithium has been shown to develop a protective solid electrolyte interphase (SEI) layer. This passivating layer plays a crucial role in determining the system's function and catalytic performance.

## 2.1 Reaction mechanisms of Li-mediated $\text{N}_2$ reduction

### 2.1.1 Chemical $\text{N}_2$ splitting and chemical protonation.

Tsuneto *et al.*<sup>6</sup> first proposed a Li-mediated route, which involves three processes (eqn (1)): (1)  $\text{Li}^+$  ions are reduced to metallic Li; (2) metallic Li reacts with  $\text{N}_2$  and breaks the robust triple bond of  $\text{N}_2$  (through a dissociative mechanism) and forms  $\text{Li}_3\text{N}$ ; (3)  $\text{Li}_3\text{N}$  reacts with an aprotic additive such as EtOH and forms  $\text{NH}_3$  and  $\text{Li}^+$  ions that dissolve back into solution.



There are two major steps involved for  $\text{N}_2$  reduction to synthesize  $\text{NH}_3$ , *i.e.*, the activation of  $\text{N}_2$  followed by its protonation. A spontaneous chemical interaction takes place between split  $\text{N}_2$  and electrodeposited Li to generate lithium nitride in the chemical  $\text{N}_2$  splitting and chemical protonation model (Fig. 2). This suggests that interactions between  $\text{N}_2$  and the electrons of metallic Li take place. Additionally, the release of  $\text{Li}^+$  into the solution occurs concurrently with the chemical protonation of activated lithium nitride to create  $\text{NH}_3$ . Activation of  $\text{N}_2$  is mainly affected by the different characteristics of Li deposition. As long as there is still active Li





Fig. 2 Mechanism of catalytic recycling of lithium intermediates. Reproduced with permission.<sup>23</sup> Copyright 2021, Wiley-VCH.

on the electrode,  $N_2$  reduction and  $NH_3$  synthesis can continue even after the current is switched off.<sup>6,11,23</sup> In this mechanism,  $N_2$  is activated and protonated mainly through chemical reactions. The only electrochemical step in this route is Li deposition. The rate-determining step was claimed to be the reaction of Li with  $N_2$ .

Likewise, Cai *et al.* provided a detailed mechanisms of  $eN_2RR$  where the majority (>99%) of the electrochemical reaction is Li deposition, while the subsequent chemical reactions of  $N_2$  activation and protonation are primarily chemical in nature (Fig. 3). They further demonstrated that another significant competing reaction is the interaction between Li deposits and THF. Substantial reactivity for  $N_2$  activation is only present in recently deposited Li. After being deactivated by THF, the newly deposited Li gradually loses its ability to reduce  $N_2$ . Therefore, protecting “fresh” metallic Li is essential to enhancing  $N_2$  reduction performance. This “fresh Li” technique also explains how performance is influenced by current density. A high level of  $NH_3$  FE and  $NH_3$  yield rate were obtained through this mechanism.<sup>40</sup>

**2.1.2  $N_2$  activation and protonation through an associative mechanism.** High energy electrons are also easily accessible at the Li-plating potential and may theoretically

electrochemically convert dissolved  $N_2$  and protons into  $NH_3$ . A Li layer might support coupled proton–electron transfers in a heterogeneous catalytic cycle. As protons and electrons are transferred in tandem, metallic  $Li^+$  should not dissolve.  $N_2$  activation and protonation can be controlled by altering the electrode surface or the applied potential when  $N_2$  activation and protonation are both electrochemical processes.<sup>40,41</sup>

Schwalbe and coworkers<sup>41</sup> combined experiment with density functional theory (DFT) modeling and revealed that plated Li could react with  $N_2$  and ethanol to form  $Li_3N$  and  $LiH$ , and that the active centers on the surfaces of Li,  $Li_3N$ , and  $LiH$  are the long-bridge site, the nitrogen vacancy, and the hydrogen vacancy, respectively.<sup>41</sup> Based on DFT calculations, they inferred that  $Li-eN_2RR$  could follow a heterogeneous mechanism (Fig. 3a).  $N_2$  is first adsorbed onto the solid surface composed of Li,  $Li_3N$ , and  $LiH$ . It is then activated on the surface and the activated  $N_2$  is protonated stepwise to form  $NH_3$ . They also showed that  $Li_3N$  is kinetically stable but not thermodynamically stable. There could therefore be a bottleneck in the diffusion of vacancies from the bulk to the surface, which limits the decomposition of  $Li_3N$  to Li and  $NH_3$ . The authors proposed plausible pathways on the surfaces of Li,  $Li_3N$ , and  $LiH$ , depicted in Fig. 3b. The necessary limiting potentials on the corresponding surfaces are  $-0.76$ ,  $-1.33$ , and  $-1.53$  V against the reversible hydrogen electrode (RHE), respectively. Before the formation of  $NH_3$ , all routes pass through adsorbed  $NH_x$ . It is essential to remember that the determination of the limiting potential makes use of the computational hydrogen electrode (CHE) assumptions.<sup>42</sup> The CHE assumes the pH of the aqueous electrolyte is known. They employed onset potential for ethanol reduction from the trials as a baseline to account for the nonaqueous electrolyte present in this experiment. The results showed that under the conditions of these trials, all three surfaces are capable of assisting in the production of  $NH_3$ .<sup>41</sup>

**2.1.3 Chemical  $N_2$  splitting and electrochemical protonation.** An alternative  $Li-eN_2RR$  mechanism involves a

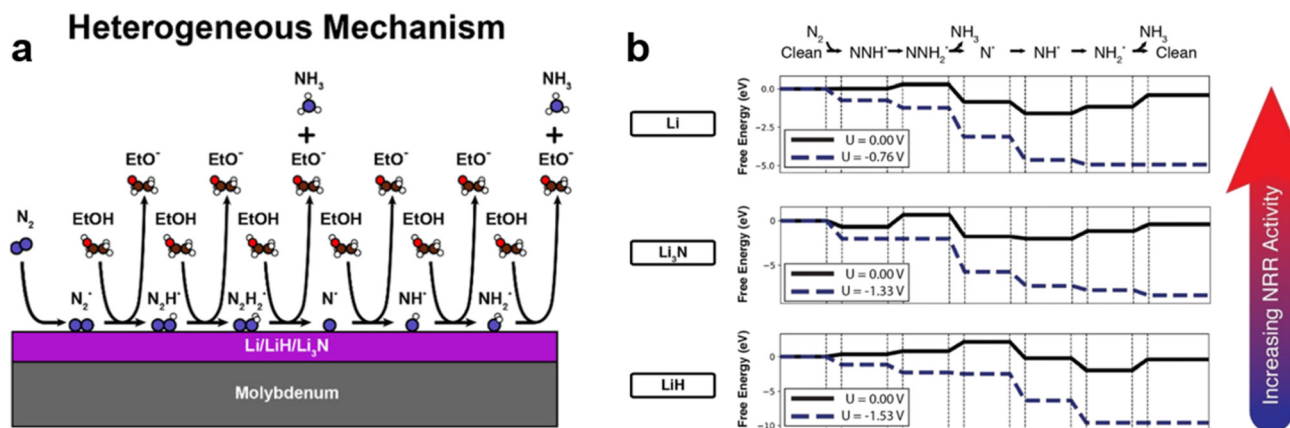


Fig. 3 (a) A ‘Heterogeneous mechanism’, in which there is a stable amount of lithium on the electrode at all times; (b) free energy diagram of  $NH_3$  formation on the surfaces of Li,  $Li_3N$ , and  $LiH$ . The free energy diagram is represented through dash lines when the limiting potential is switched on. All of these surfaces are active for  $NH_3$  synthesis.<sup>41</sup>



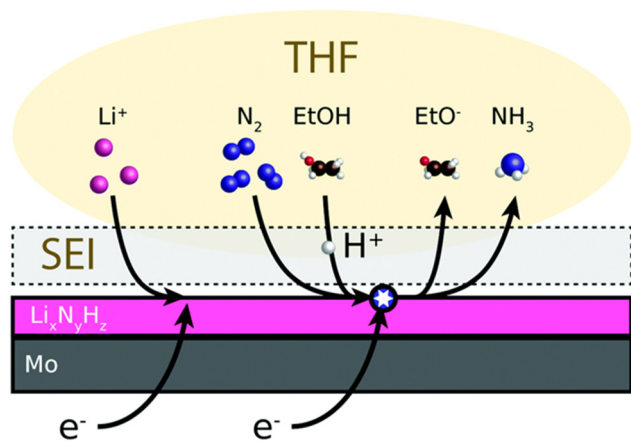


Fig. 4 Schematic of the mechanism for Li-eN<sub>2</sub>RR to NH<sub>3</sub>. A non-aqueous electrolyte (THF) contains lithium salt which is electrodeposited onto a metal electrode (Mo) as metallic Li.<sup>38</sup>

chemical process of Li<sub>3</sub>N and an electrochemical process from Li<sub>3</sub>N back to metallic Li, as presented in Fig. 4. Andersen and coworkers claimed that the active surface site of Li (Li<sup>•</sup>) can react with ethanol and activate N<sub>2</sub>. Li<sup>•</sup> was not consumed throughout the process.<sup>38</sup> This kinetic model of Li-eN<sub>2</sub>RR is consistent with the observation of a variation in NH<sub>3</sub> yield rate and FE with the change of external conditions. To explain the mechanism of Li-mediated N<sub>2</sub> reduction reaction toward NH<sub>3</sub>, the authors created a basic kinetic model. They proposed that the following fundamental actions take place during lithium deposition.



∴ s = close to surface species

∴ Li<sup>•</sup> = active surface site of Li

∴ Li<sup>•</sup>X\* = surface bound X species

Here eqn (2a) and (2b) describe the slow steps of Li-deposition, while eqn (2c)–(2e) and (2f)–(2j) show the catalytic formation of H<sub>2</sub> and NH<sub>3</sub>, respectively.

There have been several computational studies on the reaction mechanism of Li-mediated N<sub>2</sub> reduction and understanding the factors that influence the efficiency and selectivity of this process. These studies have used a variety of computational techniques, including DFT calculations, to examine the reaction pathways and intermediate species involved in the reduction of N<sub>2</sub> to NH<sub>3</sub> using lithium as a mediator. Some of the key findings from these computational studies include the importance of the choice of electrocatalyst, as different electrocatalysts have been found to have a significant impact on the reaction mechanism and efficiency of the Li-mediated N<sub>2</sub> reduction process. The formation and stability of intermediate species, such as lithium nitride and lithium amide, have been found to play a key role in the reaction mechanism of Li-mediated N<sub>2</sub> reduction. The influence of electrolytes also has significant impact on the reaction mechanism.<sup>40,43–46</sup>

Maniscalco *et al.* employed a Car-Parrinello molecular dynamics (CPMD) method to simulate the first step of Li-mediated NH<sub>3</sub> synthesis. CPMD, a type of *ab initio* molecular dynamics method (AIMD), is a classical technique, which is well known from classical molecular dynamics (or force-field) calculations, to address the challenge of how to characterize nuclear motion in a simple manner. The DFT method was employed for the studies of electronic structure and the motions in the system, which were further characterized through CPMD.<sup>47</sup>

At every step, the electronic cloud tracks the nuclei's movement. The dynamics of molecular systems on the size of a few ps and a few NH<sub>3</sub> can be described using a time interval of around 0.1 fs. Since chemical reactions are infrequent events, it is challenging to meaningfully simulate them. Before monitoring reactions, it is especially preferable to build an equilibrium system with a precise temperature. Such equilibrated systems are difficult to obtain or perhaps unattainable. The molecules of N<sub>2</sub> were those that interact with the surface the most firmly. In contrast to how molecules behave when they come in contact with oxide surfaces,<sup>48,49</sup> Maniscalco *et al.* observed that the N<sub>2</sub> molecules are quickly “swallowed” by the metallic-Li surface. Typically, this causes the nitrogen–nitrogen bond to lengthen. Most simulations showed at least one N<sub>2</sub> molecule completely dissociating.<sup>50</sup> To evaluate the eN<sub>2</sub>RR route on lithium, lithium nitride, and lithium hydride surfaces, Schwalbe *et al.* employed DFT calculations and limiting potential analysis.<sup>41</sup> Both lithium that is electrochemically attached to the electrode and lithium that is separated, where the dissolution is triggered by the loss of lithium metal to lithium ions, will be affected by this. The experimental results indicate that only a tiny portion of the lithium that is plated will react to generate a species that contains N<sub>2</sub>, which is why lithium was chosen. The thermodynamic justification



used to select nitride and hydride is described above. The final assumption from these studies is that all three surface species have plausible routes. According to previous research on nitride materials, the active site for the nitride and hydride is a vacancy.<sup>51,52</sup>

Despite their usefulness, computational methods have several limitations in understanding Li-mediated  $N_2$  reduction. One major limitation is the accuracy of the computational models and the assumptions made during the simulations. These assumptions can lead to errors and inaccuracies in the results. Additionally, some of the simulations may not capture the full complexity of the reaction mechanism or may oversimplify the system. Another limitation is the computational cost of the simulations, which can be significant, especially for large systems or long time scales. Finally, the results of computational simulations may not always be directly applicable to experimental systems, as experimental conditions may differ from the simulated conditions.

## 2.2 Cathode catalysts reported for Li-mediated $N_2$ reduction

The fixation and optimization of  $N_2$  to yield  $NH_3$  at ambient conditions is a key challenge for the field of chemical engineering.  $N_2$  fixation by several chemical as well as electrochemical systems has been employed to realize the synthesis of  $NH_3$  at mild conditions. Li metal catalysts are now well known for the electrochemical reduction of  $N_2$  to  $NH_3$  at ambient conditions.<sup>53,54</sup> The spontaneous reaction of Li with  $N_2$  yields  $Li_3N$ , and subsequent protonation of the  $Li_3N$  realizes the synthesis of  $NH_3$ . However, it is a challenge to employ Li catalysts in an aqueous solution during Li-mediated  $eN_2RR$ . When a lithium mediator is used in an aqueous solution, the competitive HER occurs at a more positive potential than that of the reduction of  $Li^+$  to Li.<sup>55–57</sup>

In 1930, Fichter *et al.*<sup>5</sup> for the first time described the Li-mediated  $eN_2RR$ . It was further extended and explored by Tsuneto *et al.* in the early 1990s. The reduction of  $N_2$  was carried out in the presence of  $LiClO_4$  (0.2 M) as an electrolyte, THF and ethanol (volume ratio of 99:1) as protic solvents and  $N_2$  at 1 atm. Different metal electrodes such as Al, Ti, Mo, Fe, Co, Ni, Cu, Ag, *etc.* were explored. The process achieved a maximum current efficiency of 8% at 1 atm. The current efficiency of the process was demonstrated to be increased up to 59% by raising the pressure of  $N_2$  to 50 atm. Moreover, the study revealed that  $NH_3$  could be generated by taking the air as the source of  $N_2$  with a current efficiency of 3.7%. The lower current efficiency was attributed to the side reaction of Li metal with  $O_2$  present in the air.<sup>6</sup>

The current efficiency of the electrochemical process was found to rely on the metals used for electrodes (especially the cathode) in addition to electrolytes, protic additives, temperature, and pressure conditions.<sup>38</sup> For practical applications, the efficiency of the Li- $eN_2RR$  process can be enhanced by the introduction of alternative cyclic strategies, surface engineering of the electrode's reactive interface, use

of gas diffusion electrodes for efficient catalysis, the possible use of ionic liquids as proton shuttles, or addition of oxygen species.<sup>22,24,38,58,59</sup> In the following section, we only focus our discussion on the state-of-the-art contributions that have demonstrated exceptional activity by optimization of the Li-mediated electrocatalytic reduction process.

### 2.2.1 Noble metal catalysts for Li-mediated $eN_2RR$

**2.2.1.1 Li-Ru composite.** Ma *et al.*<sup>60</sup> investigated  $eN_2RR$  based on a Li- $N_2$  battery using carbon-supported Ru nanoparticles as a cathode catalyst in the presence of water as a proton source.  $LiOH$  and  $NH_3$  were produced by passing  $N_2$  through the water/Ru cathode interface *via* discharge-charge cycling. The water also played an additional role in the film formation and decomposition reaction at the cathode. The Li- $N_2$  battery process provided an  $NH_3$  yield of 2.66 mg, with an  $NH_3$  FE value of 4.2% at 0.1  $mA\ cm^{-2}$ , while an  $NH_3$  yield of 4.46 mg and an  $NH_3$  FE value of 1.4% at 0.5  $mA\ cm^{-2}$  after discharging for 2 h. This study suggested the novel application of Li- $N_2$  batteries for continuous Li-mediated production of  $NH_3$  and highlighted the optimal ternary role of water as a proton source.<sup>60</sup>

**2.2.1.2 Ag wire.** In 1993, Tsuneto *et al.*<sup>61</sup> tested 12 different metal wire cathodes for  $N_2$  reduction reaction using a single compartment cell under 1 atm  $N_2$  in a solution of  $LiClO_4$  (0.2 M) in tetrahydrofuran/ethanol (99:1 v/v). Ag wire electrode was found to display the best activity with a current efficiency of about 8.4% toward  $NH_3$  formation. Larger current efficiency (48.7%) was achieved when the electrolysis was performed under a high pressure of  $N_2$  (50 atm).

**2.2.1.3 Au-coated carbon fibrous paper (Au/CP) catalyst.** Gao *et al.*<sup>23</sup> employed Au/CP as a model catalyst to investigate its electrocatalytic activity for the nonaqueous Li-mediated  $eN_2RR$  process. *In situ* XRD confirmed the transformation of lithium intermediates during the  $eN_2RR$  (Fig. 5). A faster Li electro-reduction kinetics was observed on Au/CP compared to CP cathodes. The  $Li_3N(100)$  peak gradually emerged after bubbling  $N_2$  for 5 min with Au/CP (Fig. 5e), whereas no obvious signal of  $Li_3N$  appeared with a bare CP electrode (Fig. 5k). Rapid depletion of Li and  $Li_3N$  took place (Fig. 5f) after addition of EtOH, probably resulting from  $NH_3$  formation, which was corroborated by UV/vis absorption spectroscopy and nuclear magnetic resonance measurements. Au/CP demonstrated superior activity compared with CP because Au possessed higher adsorption energy than the carbon surface. Owing to higher adsorption energy, the effective transfer of electrons from Au to  $Li^+$  lowered the catalytic barrier for Li reduction. Au/CP significantly enhanced the kinetics of Li reduction, resulting in the formation of metallic Li that critically influenced the spontaneous  $eN_2RR$  process by the formation of  $Li_3N$  and  $NH_3$ . The heterogeneous catalysis by Au/CP achieved an  $NH_3$  FE of 34.0% and  $NH_3$  yield rate of 50  $\mu g\ h^{-1}\ cm^{-2}$ .<sup>23</sup>

### 2.2.2 Nonprecious metal catalysts for Li-mediated $eN_2RR$

**2.2.2.1 Copper-based materials.** Cu does not react with Li and has been demonstrated to be a suitable cathode for Li-mediated  $eN_2RR$ . Recently, a highly structured Cu electrode





Fig. 5 *In situ* XRD contour maps of (a) and (d) Au/CP and; (g) and (j) CP under Ar atmosphere; (b) and (e) Au/CP and (h) and (k) CP under N<sub>2</sub> atmosphere without EtOH; (c) and (f) Au/CP and (i) and (l) CP under N<sub>2</sub> atmosphere with EtOH.<sup>23</sup>

on Ni foam substrates was fabricated by Li and coworkers through a hydrogen bubble template (HBT) method (Fig. 6a).<sup>58</sup> An NH<sub>3</sub> formation rate of  $46 \pm 6.8 \text{ nmol s}^{-1} \text{ cm}_{\text{geo}}^{-2}$  with a corresponding FE and energy efficiency (EE) of  $13.3 \pm 2.0\%$  and  $2.3 \pm 0.3\%$  was attained at a current density of  $-100 \text{ mA cm}_{\text{geo}}^{-2}$  under 20 bar N<sub>2</sub> using 2 M LiClO<sub>4</sub> in THF as an electrolyte and 1 vol% of EtOH as a proton source. The NH<sub>3</sub> FE and EE for HBT Cu were shown to be comparable to Cu foil (NH<sub>3</sub> FE:  $13.6\% \pm 1$ ; EE:  $3.9 \pm 0.3\%$ ), while the NH<sub>3</sub> formation rate of HBT Cu was over 45 times that of Cu foil ( $1.0 \pm 0.1 \text{ nmol s}^{-1} \text{ cm}_{\text{geo}}^{-2}$ ). It is worth noting that the synthesized HBT Cu electrode shows a great potential for scale up application compared to previously reported electrodes in terms of current density (Fig. 6b). Furthermore, an increase in salt concentration in the electrolyte was observed to lead to improved stability of the system, which may be due to suppressing the formation of a passivating decomposition layer, or it otherwise altering the SEI layer composition.

Zhang *et al.*<sup>14</sup> embedded Cu particles into lithium by sample rolling. They found that the Li in the resulting Cu/Li composite provided a reaction rate over 1000 times faster than bare Li for the lithium nitridation process (Fig. 7a and b). This was attributed to the alteration of nitrogen adsorption and decrease in the total energy required for the nitridation reaction. Reaction of Cu/Li<sub>3</sub>N with deionized water ( $2\text{Li}_3\text{N} + 3\text{H}_2\text{O} \rightarrow 2\text{NH}_3 + 6\text{LiOH}$ ) yielded NH<sub>3</sub> (Fig. 7c), which was validated by infrared spectroscopy (Fig. 7d) and Nessler's reagent spectrophotometry. The authors further compared this work with the traditional H-B process in terms of energy consumption for production of 1 kg of NH<sub>3</sub> (Fig. 7e). Taking into account that Li, Cu, and HCl are not consumed, only the costs of industrial-grade H<sub>2</sub>O and N<sub>2</sub> and the electricity employed for Li-ion reduction were considered in the calculation. The use of H<sub>2</sub>O as a hydrogen source instead of H<sub>2</sub> provides benefits for eliminating the amount of consumed fossil fuels for yielding H<sub>2</sub>, thus substantially reducing CO<sub>2</sub> emissions. The FE of this eN<sub>2</sub>RR

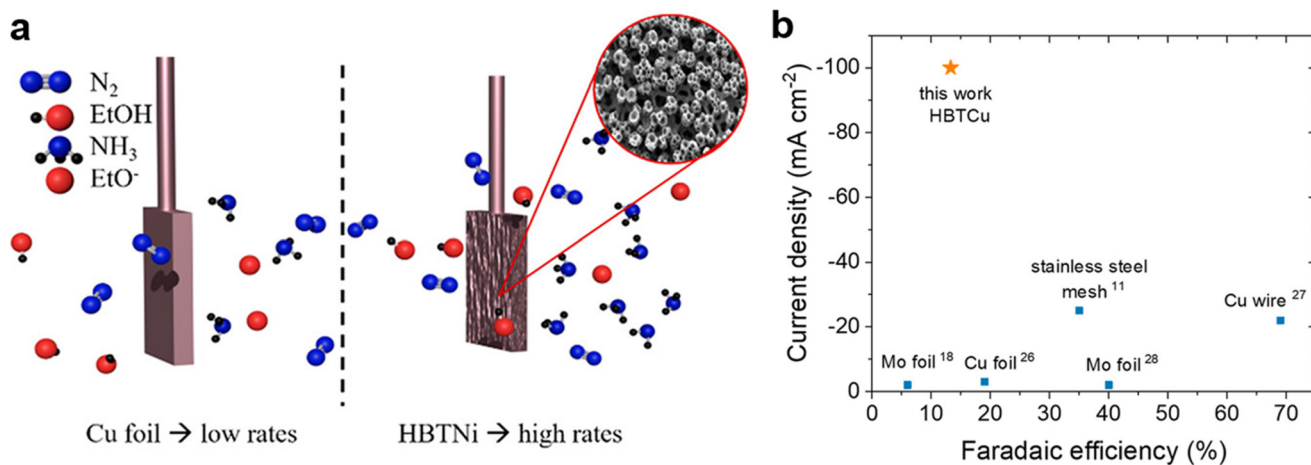
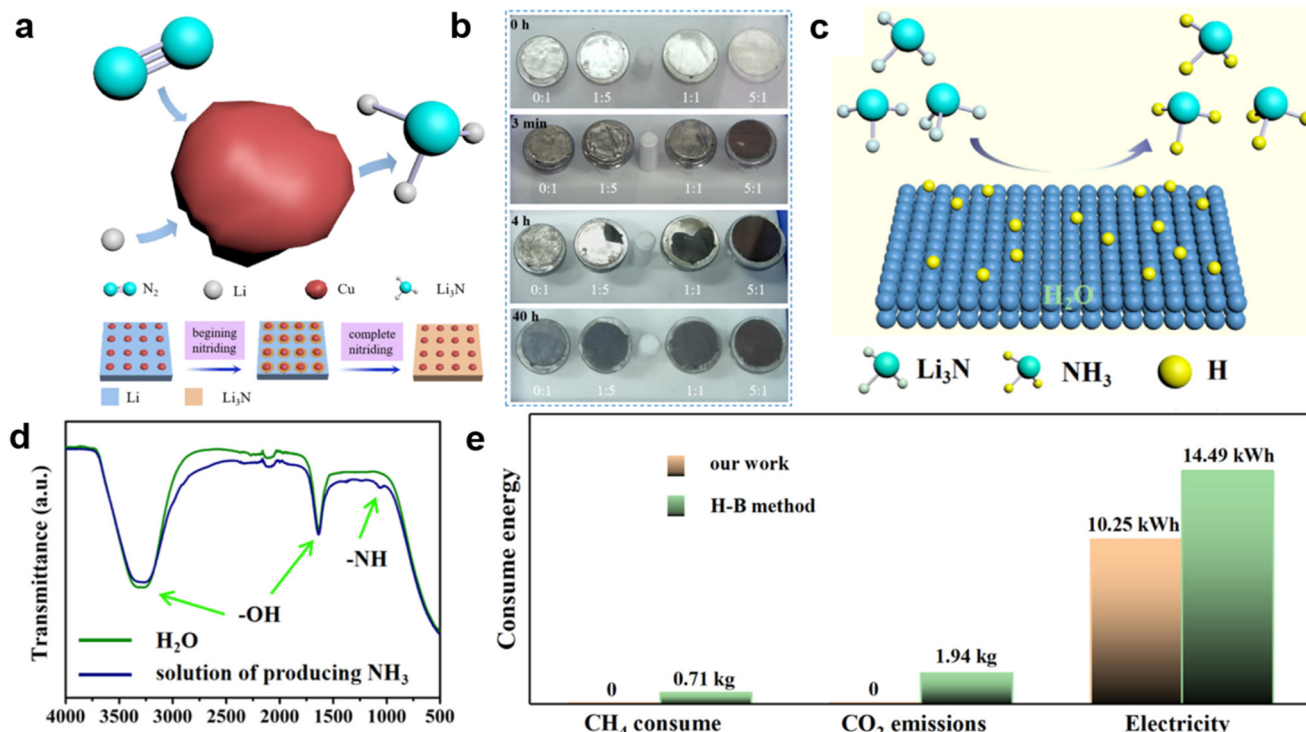


Fig. 6 (a) Illustration of Cu foil and HBT Cu for Li-mediated eN<sub>2</sub>RR; (b) comparison of HBT Cu and previously reported electrode materials in terms of current density and NH<sub>3</sub> FE.<sup>58</sup>





**Fig. 7** (a) Illustration of Cu-catalyzed lithium nitridation (top panel) and steps for the formation of Li<sub>3</sub>N/Cu from Li/Cu (bottom panel); (b) catalytic effect of Cu-to-Li mass ratio on the nitridation process; (c) illustration of NH<sub>3</sub> synthesis from the reaction of Li<sub>3</sub>N and H<sub>2</sub>O; (d) infrared spectra of H<sub>2</sub>O and the electrolyte solution after reaction; (e) comparison of this work with the H-B process in terms of energy consumption for production of 1 kg of NH<sub>3</sub>.<sup>14</sup>

fixation route using insulated solid electrolyte can reach close to 100%.

**2.2.2.2 Molybdenum (Mo).** In addition to Cu, Mo also does not alloy with Li and has been used as a cathode for Li-mediated eN<sub>2</sub>RR.<sup>6,61</sup> An NH<sub>3</sub> FE of ~10% at a current density of 100 mA cm<sup>-2</sup> was achieved on a Mo working electrode in 0.5 M LiClO<sub>4</sub> in THF with the addition of a small amount of EtOH (0 to 5 vol%).<sup>41</sup> Andersen *et al.*<sup>38</sup> reported a simple

strategy for improving the NH<sub>3</sub> FE by cycling the applied voltage between a Li deposition favored region and a Li dissolution facilitated regime (Fig. 8a and b). The NH<sub>3</sub> FE was enhanced from ~21.2% under constant Li deposition to 37% after potential cycling on a Mo electrode with 0.3 M LiClO<sub>4</sub> electrolyte in THF containing 1 vol% ethanol. Li *et al.*<sup>59</sup> discovered that the addition of a small amount of O<sub>2</sub> could greatly improve the NH<sub>3</sub> FE and stability of the

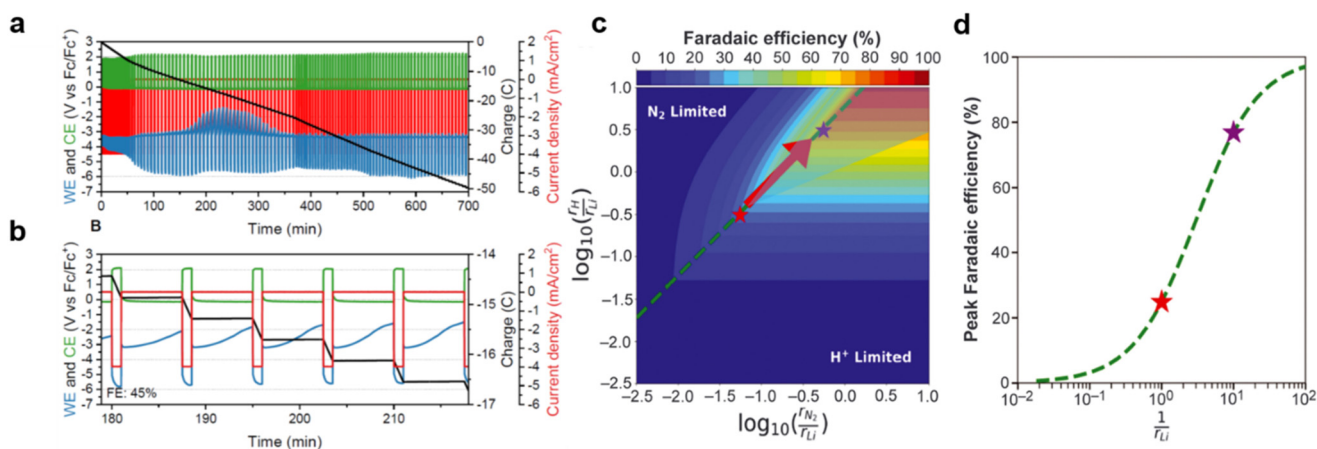


**Fig. 8** (a) Cycling method between -2.0 and 0.0 mA cm<sup>-2</sup> (red) for a total of 100C of charge passed (black); (b) a close-up of the cycling;<sup>38</sup> (c) Heatmap of the predicted FE against the ratio of N<sub>2</sub> to lithium (x axis) and proton to lithium (y axis) diffusion rates; (d) a one-dimensional plot of NH<sub>3</sub> FE cut along the optimal  $r_{N_2}/r_H$  ratio.<sup>59</sup>



lithium-mediated eN<sub>2</sub>RR. A high NH<sub>3</sub> FE of up to 78 ± 1.3% was obtained at 0.6 to 0.8 mole% O<sub>2</sub> in 20 bar of N<sub>2</sub> with 0.3 M LiClO<sub>4</sub> electrolyte in THF containing 1 vol% ethanol. The NH<sub>3</sub> FE was found to increase with the decrease of Li diffusion rate (Fig. 8c). This can be associated with the fact that Li electrodeposition competes with the N<sub>2</sub>RR for electrons. Ideally, Li diffusion or deposition should be slow enough to consume a minimal number of electrons while still providing a full monolayer of clean and freshly plated Li to dissociate N<sub>2</sub>. O<sub>2</sub>-induced changes in the SEI layer can lead to delayed Li diffusion, thereby boosting the FE toward NH<sub>3</sub>. The oxygen content also affected the rates of nitrogen and proton diffusion,  $r_{N_2}$  and  $r_H$ , due to induced modification of the SEI layer. An optimal O<sub>2</sub> content was proposed to follow as a trade-off between the Li<sup>+</sup> diffusivity limited regime and the dominant ORR (over the N<sub>2</sub>RR) regime (Fig. 8d).

**2.2.2.3 Lithium-liquid alloy-salt (Li-Sn liquid alloy & molten LiCl-KCl).** Apart from the application of solid-state electrolytes, the use of liquid alloys with molten salts have recently been reported. To overcome the limitation of the scaling relation between the activation barrier and binding energy of N<sub>2</sub>, Tang *et al.*<sup>62</sup> introduced a Li-based loop using a Li-Sn liquid alloy (having LiSn, Li<sub>7</sub>Sn<sub>3</sub>, Li<sub>5</sub>Sn<sub>2</sub>, and Li<sub>13</sub>Sn<sub>5</sub> intermetallic phases) and molten LiCl-KCl salt as a catalyst for the generation of NH<sub>3</sub> from N<sub>2</sub> and H<sub>2</sub> gases at ambient conditions. The looping process involved a three-step reaction cascade. During the first step, the Li present in Li-Sn alloy reacted with N<sub>2</sub> to form Li<sub>3</sub>N, which dissolved readily in the molten salt. In the consecutive second step, the Li<sub>3</sub>N underwent hydrogenation to yield NH<sub>3</sub> and LiH. The third step involved the decomposition of LiH and regeneration of Li metal in the presence of Sn. This looping process at 450 °C exhibited an NH<sub>3</sub> yield rate of 0.12 μg s<sup>-1</sup> during the 81 h electrocatalytic test (Fig. 9). The highest activity of this catalytic system (Li-Sn alloy and molten LiCl-KCl salt) was found to be 0.249 μmol g<sup>-1</sup> h<sup>-1</sup>, which was higher than that of pure Na but considerably lower than the looping process catalyzed by LiH/Li<sub>2</sub>NH.<sup>62</sup>

**2.2.2.4 Stainless steel cloth (SSC).** The use of conventional gas diffusion electrodes (GDEs) with non-aqueous electrolytes is hampered by the absence of hydrophobic repulsion between the solvent and carbon fibre skeleton. A recent study by Lazouski *et al.*<sup>22</sup> demonstrated an approach to overcome transport limitations in THF by using SSC as a cathode and an anode GDE substrate (Fig. 10) for Li-mediated eN<sub>2</sub>RR, giving rise to an NH<sub>3</sub> partial current density and FE of 8.8 ± 1.4 mA cm<sup>-2</sup> and 35 ± 6%, respectively. The total NH<sub>3</sub> FE did not markedly vary when the flow rate of N<sub>2</sub> across the SSC was changed; less NH<sub>3</sub> was observed in the gas phase at lower flow rates. However, the NH<sub>3</sub> formation rate decreased with electrolysis time. The reason for this degradation needs to be further explored.

### 2.2.3 Non-metal catalysts for eN<sub>2</sub>RR

**2.2.3.1 Li<sup>+</sup> incorporated poly(*N*-ethyl-benzene-1,2,4,5-tetracarboxylic diimide)-carbon cloth (Li<sup>+</sup>-PEBCD/CC).** Chen *et al.*<sup>3</sup> reported a dramatic increase in the efficiency and selectivity of the eN<sub>2</sub>RR process (at ambient conditions) by employing Li<sup>+</sup>-PEBCD/CC as the catalyst. DFT calculations as well as experimental studies verified the association of the Li<sup>+</sup> with the oxygen atoms that inhibit the HER. Further, it also facilitates the adsorption of N<sub>2</sub>, and the hydrogenation reaction proceeds in a “[O-Li<sup>+</sup>]-N<sub>2</sub>-H<sub>x</sub>” manner (Fig. 11a). The highest values of FE and NH<sub>3</sub> yield rate of 2.85% and 2.01 μg h<sup>-1</sup> cm<sup>-2</sup> were achieved at -0.5 and -0.7 V, respectively (Fig. 11b and c). The durability tests suggested 82% performance retention and stable behavior of the Li<sup>+</sup>-PEBCD/CC electrode with a slight change of FE after 6 cycles (Fig. 11d).<sup>3</sup>

**2.2.3.2 N-doped carbon nanospikes (CNS).** Song *et al.*<sup>34</sup> demonstrated the effect of N-doped CNS as a physical catalyst to promote the eN<sub>2</sub>RR. The catalyst does not contain noble or non-precious metals, but instead the sharp nanospikes of the carbon act as the electrocatalytic surface as they concentrate the electric field at the tips and catalyze the eN<sub>2</sub>RR process of the dissolved N<sub>2</sub> at the electrode. The counter ion (*i.e.*, Li<sup>+</sup>, Na<sup>+</sup>, and K<sup>+</sup>) present in the electrolyte was also observed to



Fig. 9 (a) Graphical illustration of Li-eN<sub>2</sub>RR containing Li-Sn alloy and molten LiCl-KCl salt forming a biphasic system; (b) NH<sub>3</sub> yield rate against electrolysis time on Li-Sn and pure Sn.<sup>62</sup>





Fig. 10 (a) A hydrophobic GDE with an aqueous electrolyte; (b) a hydrophobic GDE with a non-aqueous electrolyte; (c) a catalyst-coated (SSC) GDE with a non-aqueous electrolyte.<sup>22</sup>

critically influence the performance of the reaction by enhancing the electric field and  $N_2$  concentration in the Stern layer. Moreover, the CNS suppresses the HER by formation of a cation layer around the tip of the spikes, which excludes water and provides access to a high electric field to the  $N_2$  molecules. The counter-ions enhanced the  $NH_3$  production rate in the order of  $Li^+ > Na^+ > K^+$ . Using  $LiClO_4$  as an electrolyte and CNS as a catalyst, an  $NH_3$  FE,  $NH_3$  yield rate, and energy efficiency of 11.56%, 97.18  $\mu g h^{-1} cm^{-2}$ , and 5.25% were achieved, respectively.<sup>34</sup>

Among the reported catalysts for Li-mediated  $eN_2RR$ , as illustrated in Table 2, HBT Cu gives the best  $NH_3$  yield rate,

possibly due to its porous structure with high surface area benefiting the lithium-mediated process. The Cu/Li composite exhibited a 100%  $NH_3$  FE. However, the metal-free CNS demonstrated both high yield and FE toward  $NH_3$  with a corresponding value of 97.18  $\mu g h^{-1} cm^{-2}$  and 11.56%, respectively.

### 2.3 Electrolytes reported for Li-mediated $N_2$ reduction

In the electrochemical method, a proton donor is required to reduce the  $N_2$  (such as  $LiN_3$ ) so that  $NH_3$  is released and Li ions are recovered. There are reasons to think that the proton



Fig. 11 (a) The graphic illustration of the configuration of the electrochemical cell for the  $eN_2RR$  process; (b) FEs of the  $Li^+$ -PEBCD/CC catalyst at different potentials during the  $eN_2RR$ ; (c)  $NH_3$  yield rate against applied potential during the  $eN_2RR$ ; (d) durability test results for  $Li^+$ -PEBCD/CC.<sup>3</sup>



**Table 2** A summary of reported electrocatalysts for the Li-mediated eN<sub>2</sub>RR

| Sr #                        | Cathode catalyst                 | NH <sub>3</sub> FE (%) | NH <sub>3</sub> yield/NH <sub>3</sub> yield rate                                                          | Electrolyte                                                                                                              | Ref. |
|-----------------------------|----------------------------------|------------------------|-----------------------------------------------------------------------------------------------------------|--------------------------------------------------------------------------------------------------------------------------|------|
| Noble metal catalyst        |                                  |                        |                                                                                                           |                                                                                                                          |      |
| 1                           | Ru NPs@C                         | 4.2                    | 4.46 mg                                                                                                   | 1 M LiCF <sub>3</sub> SO <sub>3</sub> in TEGDME                                                                          | 60   |
| 2                           | Ag wire                          | 1.4                    | 66 mg                                                                                                     | 0.2 M LiClO <sub>4</sub> in THF with 1 vol% EtOH                                                                         | 61   |
| 3                           | Au/CP                            | 8.4                    | —                                                                                                         | 0.2 M LiClO <sub>4</sub> in THF with 1% EtOH                                                                             | 23   |
| 3                           | Au/CP                            | 34                     | 50 μg h <sup>-1</sup> cm <sup>-2</sup>                                                                    | 0.2 M LiClO <sub>4</sub> in THF with 1% EtOH                                                                             | 23   |
| Non-precious metal catalyst |                                  |                        |                                                                                                           |                                                                                                                          |      |
| 4                           | HBT Cu on Ni foam                | 13.3 ± 2               | 46 ± 6.8 nmol s <sup>-1</sup><br>cm <sub>geo</sub> <sup>-2</sup> @-100 mA cm <sub>geo</sub> <sup>-2</sup> | 2 M LiClO <sub>4</sub> in THF with 1 vol% of EtOH                                                                        | 58   |
| 5                           | Cu foil                          | 18.5 ± 2.9             | 7.9 ± 1.6 nmol s <sup>-1</sup> cm <sub>geo</sub> <sup>-2</sup>                                            | 1 M LiBF <sub>4</sub> in THF with 0.1 M EtOH                                                                             | 11   |
| 6                           | Cu/Li composite                  | 100                    | —                                                                                                         | —                                                                                                                        | 14   |
| 7                           | Mo                               | ~10                    | —                                                                                                         | 0.5 M LiClO <sub>4</sub> in THF with 1 vol% ethanol                                                                      | 41   |
| 8                           | Mo foil spot-welded with Mo wire | 21.2 ± 1.6             | —                                                                                                         | 0.3 M LiClO <sub>4</sub> in THF with 1 vol% ethanol                                                                      | 38   |
| 9                           | Mo foil spot-welded with Mo wire | 78 ± 1.3               | —                                                                                                         | 0.3 M LiClO <sub>4</sub> in THF with 1 vol% ethanol<br>(at 0.6 to 0.8 mole% O <sub>2</sub> in 20 bar of N <sub>2</sub> ) | 59   |
| 10                          | Li-Sn liquid alloy               | —                      | 0.249 μmol g <sup>-1</sup> h <sup>-1</sup>                                                                | Molten LiCl-KCl                                                                                                          | 62   |
| 11                          | SSC                              | 35 ± 6                 | —                                                                                                         | 1 M LiBF <sub>4</sub> in THF with 0.11 M EtOH                                                                            | 22   |
| Non-metal catalyst          |                                  |                        |                                                                                                           |                                                                                                                          |      |
| 12                          | Li <sup>+</sup> -PEBCD/CC        | 2.85                   | 2.01 μg h <sup>-1</sup> cm <sup>-2</sup>                                                                  | 0.5 M Li <sub>2</sub> SO <sub>4</sub> (aq)                                                                               | 3    |
| 13                          | CNS                              | 11.56                  | 97.18 μg h <sup>-1</sup> cm <sup>-2</sup>                                                                 | 0.25 M LiClO <sub>4</sub> (aq)                                                                                           | 34   |

donor's function extends beyond supplying NH<sub>3</sub> with H atoms. It may also act as the catalyst for the reaction between Li metal and N<sub>2</sub> gas. The thermodynamic activity of the proton donor is significant for selective continuous N<sub>2</sub> reduction, according to a theoretical study of general eN<sub>2</sub>RR.<sup>6</sup> In a previous assessment of proton donors, it was found that the identification of the proton donor can significantly alter the NH<sub>3</sub> yields in the Li-mediated N<sub>2</sub> reduction process.<sup>8</sup> The proton donor is the source of hydrogen that is necessary for NH<sub>3</sub> formation from N<sub>2</sub> in Li-eN<sub>2</sub>RR.

Notably, the electrolyte plays a key role and provides an ideal environment for any electrochemical reactions to take place. However, obtaining a high yield and production rate of NH<sub>3</sub> during electrochemical synthesis is seriously hampered by the problem of N<sub>2</sub> solubility in traditional aqueous electrolytes. Thus, the most crucial problem must be resolved, namely, the dissolution of a useful concentration of N<sub>2</sub> molecules into the electrolyte so that they are accessible to the catalyst surface for their subsequent reduction.<sup>63</sup> Ren and co-workers have recently reviewed the N<sub>2</sub>RR literature, and found that most of the work (90.7%) has been done on catalyst development and only 4.7% on electrolytes.<sup>64</sup> Below are some of the recently used electrolytes for Li-mediated eN<sub>2</sub>RR.

**2.3.1 Lithium triflate (Li(CF<sub>3</sub>SO<sub>3</sub>)).** In an early work reported by Tsuneto *et al.*,<sup>6</sup> five different electrolytes (*i.e.*, LiClO<sub>4</sub>, LiBF<sub>4</sub>, Li(CF<sub>3</sub>SO<sub>3</sub>), NaClO<sub>4</sub>, and Bu<sub>4</sub>NClO<sub>4</sub>) were compared for eN<sub>2</sub>RR under 50 atm nitrogen on Cu cathode. The FE of NH<sub>3</sub> synthesis was found to increase to more than 40% when lithium salts were used as electrolyte. While NaClO<sub>4</sub> and Bu<sub>4</sub>NClO<sub>4</sub> only generated negligible amounts of NH<sub>3</sub>. Among the three Li-based salts employed in the experiment, Li(CF<sub>3</sub>SO<sub>3</sub>) afforded the best FE of 59.8% for NH<sub>3</sub> formation.

**2.3.2 Molten LiOH.** The electrochemical process in aqueous conditions is considered to limit the efficiency of NH<sub>3</sub> formation due to the competitive and dominant HER. To circumvent the HER and attain selective nitrogen reduction, McEnaney *et al.*<sup>1</sup> in 2017 reported a novel stepwise pathway for the synthesis of NH<sub>3</sub> from N<sub>2</sub> and H<sub>2</sub>O at ambient conditions (22–100 °C, atmospheric pressure) using molten LiOH as the electrolyte *via* an electrochemical lithium cycling process. The three-step reaction sequence involves LiOH electrolysis (6LiOH → 6Li + 3H<sub>2</sub>O + 3/2O<sub>2</sub>), nitridation of Li (6Li + N<sub>2</sub> → 2Li<sub>3</sub>N), and hydrolysis of Li<sub>3</sub>N (2Li<sub>3</sub>N + 6H<sub>2</sub>O → 6LiOH + 2NH<sub>3</sub>) to realize the formation of NH<sub>3</sub> with a high current efficiency of 88.5%. The formation of NH<sub>3</sub> is an exothermic process that regenerates LiOH and completes the cycle. This stepwise route prevents direct N<sub>2</sub> protonation, which significantly reduces the undesirable HER and results in a high initial current efficiency of 88.5%. The fundamental features of the cycle are the straightforward dissociation of the robust N≡N bond over metallic Li and the diffusion processes that results in Li<sub>3</sub>N at ambient temperature. The reaction was performed with an overnight N<sub>2</sub> flow (12 h) and resulted in complete conversion to nitride regardless of the temperature used (within the 22–100 °C), which further resulted in ~100% conversion efficiency to NH<sub>3</sub>.<sup>1</sup>

**2.3.3 Molten LiCl-KCl-Li<sub>3</sub>N.** Ito *et al.* discovered that azide ion (N<sup>3-</sup>) synthesis from N<sub>2</sub> could be obtained electrochemically through a molten LiCl-KCl-Li<sub>3</sub>N eutectic melt system,<sup>65</sup> which was then used for electrochemical NH<sub>3</sub> synthesis. The reactions that take place at the cathode (eqn (3)) and anode (eqn (4)) are as follows:

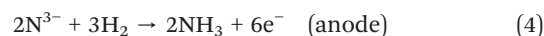




Fig. 12 (a) NH<sub>3</sub> yield and (b) NH<sub>3</sub> FE in the presence and absence of 0.03 M CsClO<sub>4</sub> at 220 °C over time.<sup>8</sup>

In the molten electrolytes, the efficiency of NH<sub>3</sub> synthesis was found to depend upon the partial pressure of hydrogen, and the dissolution/diffusion of hydrogen is the rate-determining step.

**2.3.4 Cesium salt (CsClO<sub>4</sub>).** Kim *et al.*<sup>8</sup> found that during NH<sub>3</sub> formation the Li-plating morphology plays a significant role in controlling the NH<sub>3</sub> FE. The addition of CsClO<sub>4</sub> (0.03 M) in propylene carbonate (organic electrolyte) enhanced the morphology of the Li plating, which suppressed the side reactions occurring between Li metal and propylene carbonate. With the introduction of cesium salt, the FE of the Li-mediated NH<sub>3</sub> synthesis increased up to 82.3% (Fig. 12). The performance of the thicker Li plating, plated in a cylindrical form, meant there was less total interfacial area exposed to cause side reactions.<sup>8</sup>

**2.3.5 LiClO<sub>4</sub>-poly(methyl methacrylate) (PMMA) composite.** To overcome the limitation of electrodeposition

of Li during the Li-mediated NH<sub>3</sub> synthesis at a higher temperature, Kim *et al.*<sup>66</sup> in 2019 introduced a membrane-free approach for electrodeposition of Li under ambient conditions which could be used for an enhanced nitridation reaction followed by NH<sub>3</sub> synthesis. The membrane-free biphasic system is based on the immiscible organic-aqueous hybrid electrolyte system. The biphasic hybrid electrolyte system consisted of aqueous LiClO<sub>4</sub> (1 M) and LiClO<sub>4</sub> in propylene carbonate incorporated with PMMA (1 M) that acted as a LISICON-based cell. The stable biphasic system at 5 mA cm<sup>-2</sup> required a lower operating voltage of 5.3 V, as compared with the 6.2 V required for the LISICON-based cell. This strategy afforded an NH<sub>3</sub> FE of up to 57.2 with an NH<sub>3</sub> yield of 1.21 × 10<sup>-9</sup> mol cm<sup>-2</sup> s<sup>-1</sup> (Fig. 13). This approach provides a way to design next-generation energy storage devices. By using biphasic electrolytes having high stability



Fig. 13 (a) Schematic diagram and (b) NH<sub>3</sub> yield and FE of the biphasic hybrid catalytic system catalyzed by LiClO<sub>4</sub> (aq) and LiClO<sub>4</sub>-PMMA composite.<sup>66</sup>

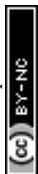




Fig. 14 (a) Schematic illustration of eN<sub>2</sub>RR catalysis using a phosphonium salt; (b) NH<sub>3</sub> yield and FE as a function of time.<sup>24</sup>

against Li, solid electrolyte interphase formation could be alleviated.<sup>66</sup>

**2.3.6 Phosphonium salt [P<sub>6,6,6,14</sub>]<sup>+</sup>.** Li-mediated eN<sub>2</sub>RR requires sacrificial proton sources to thwart the competing side reactions. Recently, Suryanto *et al.*<sup>24</sup> demonstrated the use of phosphonium salt as a proton shuttle. It was found that the phosphonium cation [P<sub>6,6,6,14</sub>]<sup>+</sup> meets the criteria to act as a proton shuttle, and also exhibits an enhanced ionic conductivity that enables a robust synthetic route to synthesize NH<sub>3</sub> from N<sub>2</sub> (19.5 bar) and H<sub>2</sub> (0.5 bar) *via* a Li-mediated eN<sub>2</sub>RR. The use of phosphonium salt allowed Suryanto *et al.* to attain a high NH<sub>3</sub> yield rate of 60 (nmol cm<sup>-2</sup> s<sup>-1</sup>) and a FE of 78% during 20 h of electrolysis, which was previously unachievable (Fig. 14).<sup>24</sup>

**2.3.7 Imide-based lithium salt (LiNTf<sub>2</sub>).** A significant contribution toward the improvement of the NH<sub>3</sub> synthesis *via* the eN<sub>2</sub>RR was made by Du *et al.*<sup>67</sup> in 2022. They demonstrated an efficient, robust, and flexible pathway for the synthesis of NH<sub>3</sub> that utilizes compact ionic layering at the electrode–electrode interface. An imide-based Li-salt, LiNTf<sub>2</sub>, was used as an electrolyte, affording an NH<sub>3</sub> yield (3.9 mmol) at a high rate of 223 nmol cm<sup>-2</sup> s<sup>-1</sup> (average NH<sub>3</sub> yield rate) and 150 nmol cm<sup>-2</sup> s<sup>-1</sup> (stabilized NH<sub>3</sub> yield rate after 24 h) with a FE of 99% and a current-to-NH<sub>3</sub> efficiency rate of approximately 100%. The ionic assembly formed at the electrode–electrode interface hampers the decomposition of the electrolyte and improves the performance by supporting stable N<sub>2</sub> reduction.<sup>67</sup>

### 3 Conclusions and future remarks

This review has focused on the considerable advancements during recent years toward the development of a sustainable and green eN<sub>2</sub>RR process. Li-mediated eN<sub>2</sub>RR performance such as NH<sub>3</sub> yield, FE, current to NH<sub>3</sub> efficiency rate, *etc.*, is low when aqueous electrolytes are used at ambient temperature and pressure conditions due to competitive reactions. We have critically discussed the main factors such as the nature of electrolyte, the material of the electrode, and mechanisms involved in the Li-mediated eN<sub>2</sub>RR. The mechanistic understanding derived through investigation of

the various factors that play a vital role in governing the performance parameters will help guide the search for the technological solutions for the current challenges in eN<sub>2</sub>RR catalysis.

The main challenge for the Li-mediated eN<sub>2</sub>RR process is to design selective electrocatalysts that can boost the activation of N<sub>2</sub> and hydrogenation to afford NH<sub>3</sub> by actively controlling the mass and charge transport during the process.<sup>38</sup> Non-aqueous solvents and different salts as electrolytes have been used to ameliorate the competing HER side reaction,<sup>68</sup> with Li-mediated N<sub>2</sub> reduction in non-aqueous electrolytes exhibiting a high NH<sub>3</sub> yield rate and FE. However, some other serious challenges such as high overpotential, unsustainable proton source from sacrificial solvent, a large ohmic resistance, and organic solvent recovery have arisen.<sup>22,64,69–72</sup>

To overcome the existing limitations and challenges of Li-eN<sub>2</sub>RR systems, we propose the following strategies to improve the efficiency of the process: the overpotential for Li<sup>+</sup> electrodeposition could be lowered by use of either active Li or its alloys with other metals, which deserves further exploration for N<sub>2</sub> activation.<sup>70,72</sup> Besides, alternative liquid electrolytes should be investigated for use in Li-mediated eN<sub>2</sub>RR systems, and the mechanisms of electrolyte decomposition should be explored to avoid the use of conventional low boiling organic electrolytes (*e.g.*, THF).<sup>71,73,74</sup> Most of the Li-mediated eN<sub>2</sub>RR process have been investigated in a batch-type electrochemical cell (*i.e.*, a single compartment or an autoclave), which suffers from the limitation of mass transport due to the low solubility of both N<sub>2</sub> and H<sub>2</sub> in liquid electrolytes. The limitation of mass transport can be resolved by using continuous-flow electrolyzers to significantly enhance the rate of N<sub>2</sub> reduction by providing gaseous reactants at the catalytic surface (Fig. 15a).<sup>41,75–77</sup> Solid state electrolytes can be implemented to realize the selective and efficient synthesis of NH<sub>3</sub> at ambient temperature and pressure. To realize electrosynthesis of NH<sub>3</sub> at industrial scale, gas diffusion electrodes should be used to continuously providing gaseous reactants to the catalytic active sites. Flow cells and membrane electrode assembly (MEA) electrolyzers should be



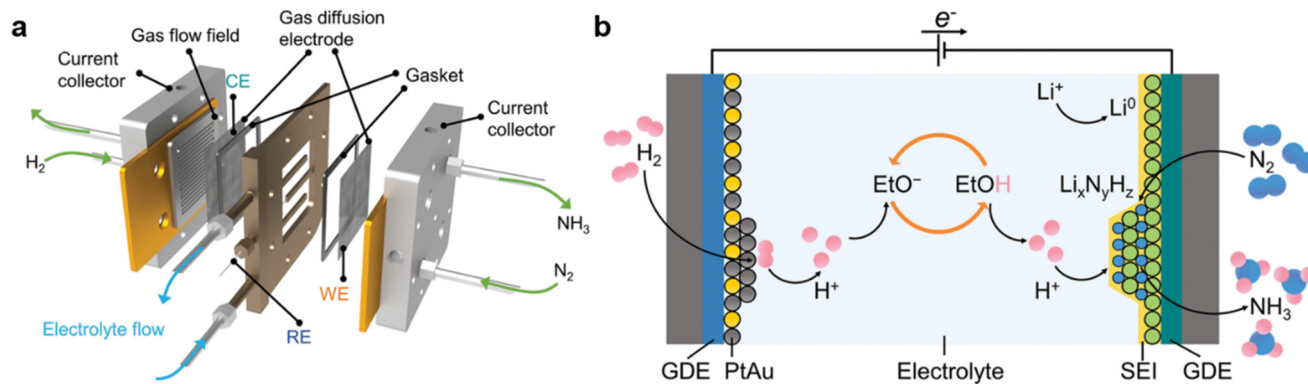


Fig. 15 (a) Expanded view of the continuous-flow electrolyzer configuration; (b) schematic process of the Li-NRR in a continuous-flow electrolyzer.<sup>72</sup>

designed and optimized that could significantly enhance the rate of eN<sub>2</sub>RR.<sup>56,76,77</sup>

The eN<sub>2</sub>RR process requires a proton donor which plays a crucial role in the production of NH<sub>3</sub> via N<sub>2</sub> reduction. A variety of proton donors have been shown to promote the reaction, and the donor's capacity to boost the reaction significantly depends on the proton donor structure and concentration. The proton donors induce changes in the solid electrolyte interphase, thereby facilitating selective diffusion of N<sub>2</sub> species to active sites on the electrode for reduction.<sup>68</sup> Hence, solid electrolyte interphases can enhance the selectivity as well as NH<sub>3</sub> yield by accelerating the homogenous deposition of lithium, as well as hindering the HER and uncontrolled electrolyte decomposition reactions. Lithium fluoride-based electrolytes have been found to achieve high selectivity due to the formation of a fluoride-rich SEI.<sup>72</sup> Note that most eN<sub>2</sub>RR studies applied a sacrificial solvent as a proton donor, which leads to difficulty in scaling up fabrication in batch reactors. To circumvent this issue, employing a hydrogen oxidation reaction (HOR) on the anode (with the hydrogen sourced from water splitting) appears to be a promising strategy to provide a sustainable hydrogen source for NH<sub>3</sub> production (Fig. 15b). To this end, the design and development of active and robust HOR anode materials (such as PtAu) in organic electrolytes for replacing the archetype Pt is crucial.

More efforts are suggested to be devoted to conducting deep mechanistic investigations.<sup>78</sup> Along with experimental studies, theoretical calculations in combination with *in situ/operando* analysis using advanced techniques could help reveal the phase changes, reaction pathways, and insights into the composition of the SEI layer and its interaction with adsorbed surface species.<sup>79,80</sup> This will aid in the rational design of efficient Li-eN<sub>2</sub>RR systems for practical applications at ambient conditions.<sup>81–85</sup>

Among others, standard protocols should be developed for accurate quantification of the N<sub>2</sub>RR process. This is crucial to tackle the problem of false positives due to the presence of N<sub>2</sub> species from several other sources such as the solvent, electrolyte, or the catalyst itself. It should be ensured through a rigorous procedure (*i.e.*, gas purification and quantitative isotope measurements) that the only N<sub>2</sub> species that are

utilized to yield NH<sub>3</sub> via the eN<sub>2</sub>RR should be the N<sub>2</sub> reactant itself so that the catalyst efficiency can be estimated with accuracy.<sup>86</sup> Due to the emerging eN<sub>2</sub>RR, we believe that the sustainable and green synthesis of NH<sub>3</sub> will be extended for practical implementation in industry in the near future, which will bring a revolution in NH<sub>3</sub>-based energy storage and conversion materials/devices.<sup>87</sup>

## Conflicts of interest

The authors declare that they have no conflict of interest.

## Acknowledgements

This work was supported by the National Natural Science Foundation of China (no. 21972010), National Key Research and Development Program of China (No. 2022YFC2105900), and Beijing Natural Science Foundation (no. 2192039).

## References

- J. M. McEnaney, A. R. Singh, J. A. Schwalbe, J. Kibsgaard, J. C. Lin, M. Cargnello, T. F. Jaramillo and J. K. Nørskov, Ammonia synthesis from N<sub>2</sub> and H<sub>2</sub>O using a lithium cycling electrification strategy at atmospheric pressure, *Energy Environ. Sci.*, 2017, **10**, 1621–1630.
- Ammonia Market (By Product Form: Liquid, Gas, Powder; By Application: Fertilizers, Refrigerants, Pharmaceuticals, Textile, Others) – Global Industry Analysis, Size, Share, Growth, Trends, Regional Outlook, and Forecast 2022–2030.
- G.-F. Chen, X. Cao, S. Wu, X. Zeng, L.-X. Ding, M. Zhu and H. Wang, Ammonia electro-synthesis with high selectivity under ambient conditions via a Li<sup>+</sup> incorporation strategy, *J. Am. Chem. Soc.*, 2017, **139**, 9771–9774.
- S. Chen, S. Perathoner, C. Ampelli, C. Mebrahtu, D. Su and G. Centi, Room-temperature electrocatalytic synthesis of NH<sub>3</sub> from H<sub>2</sub>O and N<sub>2</sub> in a gas-liquid-solid three-phase reactor, *ACS Sustainable Chem. Eng.*, 2017, **5**, 7393–7400.
- F. Fichter, P. Girard and H. Erlenmeyer, Elektrolytische bindung von komprimiertem stickstoff bei gewöhnlicher temperatur, *Helv. Chim. Acta*, 1930, **13**, 1228–1236.



- 6 A. Tsuneto, A. Kudo and T. Sakata, Lithium-mediated electrochemical reduction of high pressure N<sub>2</sub> to NH<sub>3</sub>, *J. Electroanal. Chem.*, 1994, **367**, 183–188.
- 7 H. K. Lee, C. S. L. Koh, Y. H. Lee, C. Liu, I. Y. Phang, X. Han, C.-K. Tsung and X. Y. Ling, Favoring the unfavored: Selective electrochemical nitrogen fixation using a reticular chemistry approach, *Sci. Adv.*, 2018, **4**, eaar3208.
- 8 K. Kim, H. Cho, S. H. Jeon, S. J. Lee, C.-Y. Yoo, J.-N. Kim, J. W. Choi, H. C. Yoon and J.-I. Han, Lithium-Mediated ammonia electro-synthesis: effect of CsClO<sub>4</sub> on lithium plating efficiency and ammonia synthesis, *J. Electrochem. Soc.*, 2018, **165**, F1027–F1031.
- 9 Q. Wang, J. Guo and P. Chen, Recent progress towards mild-condition ammonia synthesis, *J. Energy Chem.*, 2019, **36**, 25–36.
- 10 V. S. Marakatti and E. M. Gaigneaux, Recent advances in heterogeneous catalysis for ammonia synthesis, *ChemCatChem*, 2020, **12**, 5838–5857.
- 11 N. Lazouski, Z. J. Schiffer, K. Williams and K. Manthiram, Understanding continuous lithium-mediated electrochemical nitrogen reduction, *Joule*, 2019, **3**, 1127–1139.
- 12 R. Sažinas, K. Li, S. Z. Andersen, M. Saccoccio, S. Li, J. B. Pedersen, J. Kibsgaard, P. C. K. Vesborg, D. Chakraborty and I. Chorkendorff, Oxygen-enhanced chemical stability of lithium-mediated electrochemical ammonia synthesis, *J. Phys. Chem. Lett.*, 2022, **13**, 4605–4611.
- 13 K. Krempel, J. B. Pedersen, J. Kibsgaard, P. C. K. Vesborg and I. Chorkendorff, Electrolyte acidification from anode reactions during lithium mediated ammonia synthesis, *Electrochem. Commun.*, 2022, **134**, 107186.
- 14 Z. Zhang, Y. Zhao, B. Sun, J. Xu, Q. Jin, H. Lu, N. Lyu, Z.-M. Dang and Y. Jin, Copper particle-enhanced lithium-mediated synthesis of green ammonia from water and nitrogen, *ACS Appl. Mater. Interfaces*, 2022, **14**, 19419–19425.
- 15 R. Subbaraman, D. Tripkovic, D. Strmcnik, K.-C. Chang, M. Uchimura, A. P. Paulikas, V. Stamenkovic and N. M. Markovic, Enhancing hydrogen evolution activity in water splitting by tailoring Li<sup>+</sup>-Ni(OH)<sub>2</sub>-Pt interfaces, *Science*, 2011, **334**, 1256–1260.
- 16 A. Guha, S. Narayanaru and T. N. Narayanan, Tuning the hydrogen evolution reaction on metals by lithium salt, *ACS Appl. Energy Mater.*, 2018, **1**, 7116–7122.
- 17 M.-M. Shi, D. Bao, S.-J. Li, B.-R. Wulan, J.-M. Yan and Q. Jiang, Anchoring PdCu amorphous nanocluster on graphene for electrochemical reduction of N<sub>2</sub> to NH<sub>3</sub> under ambient conditions in aqueous solution, *Adv. Energy Mater.*, 2018, **8**, 1800124.
- 18 L. Zhang, X. Ji, X. Ren, Y. Ma, X. Shi, Z. Tian, A. M. Asiri, L. Chen, B. Tang and X. Sun, Electrochemical ammonia synthesis via nitrogen reduction reaction on a MoS<sub>2</sub> catalyst: theoretical and experimental studies, *Adv. Mater.*, 2018, **30**, 1800191.
- 19 E. Skúlason, T. Bligaard, S. Gudmundsdóttir, F. Studt, J. Rossmeisl, F. Abild-Pedersen, T. Vegge, H. Jónsson and J. K. Nørskov, A theoretical evaluation of possible transition metal electro-catalysts for N<sub>2</sub> reduction, *Phys. Chem. Chem. Phys.*, 2012, **14**, 1235–1245.
- 20 B. H. R. Suryanto, C. S. M. Kang, D. Wang, C. Xiao, F. Zhou, L. M. Azofra, L. Cavallo, X. Zhang and D. R. MacFarlane, Rational electrode–electrolyte design for efficient ammonia electrosynthesis under ambient conditions, *ACS Energy Lett.*, 2018, **3**, 1219–1224.
- 21 J. Yang, W. Weng and W. Xiao, Electrochemical synthesis of ammonia in molten salts, *J. Energy Chem.*, 2020, **43**, 195–207.
- 22 N. Lazouski, M. Chung, K. Williams, M. L. Gala and K. Manthiram, Non-aqueous gas diffusion electrodes for rapid ammonia synthesis from nitrogen and water-splitting-derived hydrogen, *Nat. Catal.*, 2020, **3**, 463–469.
- 23 L. Gao, Y. Cao, C. Wang, X. Yu, W. Li, Y. Zhou, B. Wang, Y. Yao, C. Wu, W. Luo and Z. Zou, Domino effect: Gold electrocatalyzing lithium reduction to accelerate nitrogen fixation, *Angew. Chem.*, 2021, **133**, 5317–5321.
- 24 B. H. R. Suryanto, K. Matuszek, J. Choi, R. Y. Hodgetts, H.-L. Du, J. M. Bakker, C. S. M. Kang, P. V. Cherepanov, A. N. Simonov and D. R. MacFarlane, Nitrogen reduction to ammonia at high efficiency and rates based on a phosphonium proton shuttle, *Science*, 2021, **372**, 1187–1191.
- 25 A. Jain, H. Miyaoka, S. Kumar, T. Ichikawa and Y. Kojima, A new synthesis route of ammonia production through hydrolysis of metal–nitrides, *Int. J. Hydrogen Energy*, 2017, **42**, 24897–24903.
- 26 T. Yamaguchi, K. Shinzato, K. Yamamoto, Y. Wang, Y. Nakagawa, S. Isobe, T. Ichikawa, H. Miyaoka and T. Ichikawa, Pseudo catalytic ammonia synthesis by lithium–tin alloy, *Int. J. Hydrogen Energy*, 2020, **45**, 6806–6812.
- 27 F. Chang, Y. Guan, X. Chang, J. Guo, P. Wang, W. Gao, G. Wu, J. Zheng, X. Li and P. Chen, Alkali and alkaline earth hydrides-driven N<sub>2</sub> activation and transformation over Mn nitride catalyst, *J. Am. Chem. Soc.*, 2018, **140**, 14799–14806.
- 28 Y. Gong, H. Li, J. Wu, X. Song, X. Yang, X. Bao, X. Han, M. Kitano, J. Wang and H. Hosono, Unique catalytic mechanism for Ru-loaded ternary intermetallic electrides for ammonia synthesis, *J. Am. Chem. Soc.*, 2022, **144**, 8683–8692.
- 29 P. Wang, F. Chang, W. Gao, J. Guo, G. Wu, T. He and P. Chen, Breaking scaling relations to achieve low-temperature ammonia synthesis through LiH-mediated nitrogen transfer and hydrogenation, *Nat. Chem.*, 2017, **9**, 64–70.
- 30 W. Gao, J. Guo, P. Wang, Q. Wang, F. Chang, Q. Pei, W. Zhang, L. Liu and P. Chen, Production of ammonia via a chemical looping process based on metal imides as nitrogen carriers, *Nat. Energy*, 2018, **3**, 1067–1075.
- 31 A. Sclafani, V. Augugliaro and M. Schiavello, Dinitrogen electrochemical reduction to ammonia over Iron cathode in aqueous medium, *J. Electrochem. Soc.*, 1983, **130**, 734–736.
- 32 S. Chen, S. Perathoner, C. Ampelli, C. Mebrahtu, D. Su and G. Centi, Electrocatalytic synthesis of ammonia at room temperature and atmospheric pressure from water and nitrogen on a carbon-nanotube-based electrocatalyst, *Angew. Chem., Int. Ed.*, 2017, **56**, 2699–2703.



- 33 M. Nazemi, S. R. Panikkanvalappil and M. A. El-Sayed, Enhancing the rate of electrochemical nitrogen reduction reaction for ammonia synthesis under ambient conditions using hollow gold nanocages, *Nano Energy*, 2018, **49**, 316–323.
- 34 Y. Song, D. Johnson, R. Peng, D. K. Hensley, P. V. Bonnesen, L. Liang, J. Huang, F. Yang, F. Zhang, R. Qiao, A. P. Baddorf, T. J. Tschaplinski, N. L. Engle, M. C. Hatzell, Z. Wu, D. A. Cullen, H. M. Meyer, B. G. Sumpter and A. J. Rondinone, A physical catalyst for the electrolysis of nitrogen to ammonia, *Sci. Adv.*, 2018, **4**, e1700336.
- 35 H. Mikosch, E. L. Uzunova and G. St. Nikolov, Interaction of molecular nitrogen and oxygen with extraframework cations in zeolites with double six-membered rings of oxygen-bridged silicon and aluminum atoms: A DFT study, *J. Phys. Chem. B*, 2005, **109**, 11119–11125.
- 36 S. Giddey, S. P. S. Badwal and A. Kulkarni, Review of electrochemical ammonia production technologies and materials, *Int. J. Hydrogen Energy*, 2013, **38**, 14576–14594.
- 37 Z. Yu, Y. Cui and Z. Bao, Design principles of artificial solid electrolyte interphases for lithium-metal anodes, *Cell Rep. Phys. Sci.*, 2020, **1**, 100119.
- 38 S. Z. Andersen, M. J. Statt, V. J. Bukas, S. G. Shapel, J. B. Pedersen, K. Krempel, M. Saccoccio, D. Chakraborty, J. Kibsgaard, P. C. K. Vesborg, J. Nørskov and I. Chorkendorff, Increasing stability, efficiency, and fundamental understanding of lithium-mediated electrochemical nitrogen reduction, *Energy Environ. Sci.*, 2020, **13**, 4291–4300.
- 39 J. H. Montoya, C. Tsai, A. Vojvodic and J. K. Nørskov, The challenge of electrochemical ammonia synthesis: a new perspective on the role of nitrogen scaling relations, *ChemSusChem*, 2015, **8**, 2180–2186.
- 40 X. Cai, C. Fu, H. Iriawan, F. Yang, A. Wu, L. Luo, S. Shen, G. Wei, Y. Shao-Horn and J. Zhang, Lithium-mediated electrochemical nitrogen reduction: Mechanistic insights to enhance performance, *iScience*, 2021, **24**, 103105.
- 41 J. A. Schwalbe, M. J. Statt, C. Chosy, A. R. Singh, B. A. Rohr, A. C. Nielander, S. Z. Andersen, J. M. McEnaney, J. G. Baker, T. F. Jaramillo, J. K. Nørskov and M. Cargnello, A combined theory-experiment analysis of the surface species in lithium-mediated  $\text{NH}_3$  Electrosynthesis, *ChemElectroChem*, 2020, **7**, 1542–1549.
- 42 J. K. Nørskov, J. Rossmeisl, A. Logadottir, L. Lindqvist, J. R. Kitchin, T. Bligaard and H. Jónsson, Origin of the overpotential for oxygen reduction at a fuel-cell cathode, *J. Phys. Chem. B*, 2004, **108**, 17886–17892.
- 43 O. Westhead, M. Spry, Z. Shen, A. Bagger, H. Yadegari, S. Favero, R. Tort, M. Titirici, M. Ryan, R. Jervis, A. Aguadero, J. Douglas, A. Regoutz, A. Grimaud and I. E. L. Stephens, Solvation and stability in lithium-mediated nitrogen reduction, *Meat. Abstr.*, 2022, **MA2022-02**, 1929.
- 44 O. Westhead, M. Spry, A. Bagger, Z. Shen, H. Yadegari, S. Favero, R. Tort, M. Titirici, M. P. Ryan, R. Jervis, Y. Katayama, A. Aguadero, A. Regoutz, A. Grimaud and I. E. L. Stephens, The role of ion solvation in lithium mediated nitrogen reduction, *J. Mater. Chem. A*, 2023, DOI: [10.1039/D2TA07686A](https://doi.org/10.1039/D2TA07686A).
- 45 D. Ma, Z. Zeng, L. Liu, X. Huang and Y. Jia, Computational evaluation of electrocatalytic nitrogen reduction on TM single-, double-, and triple-atom catalysts (TM = Mn, Fe, Co, Ni) based on graphdiyne monolayers, *J. Phys. Chem. C*, 2019, **123**, 19066–19076.
- 46 H. Dong, W. Xu, J. Xie, Y. Ding, Q. Wang and L. Zhou, Computational screening on two-dimensional metal-embedded poly-phthalocyanine as cathode catalysts in lithium-nitrogen batteries, *Appl. Surf. Sci.*, 2022, **604**, 154507.
- 47 D. Maniscalco, D. A. Rudolph, E. Nadimi and I. Frank, The first reaction steps of lithium-mediated ammonia synthesis: Ab Initio Simulation, *Nitrogen*, 2022, **3**, 404–413.
- 48 H. Tachikawa, Mechanism of dissolution of a lithium salt in an electrolytic solvent in a lithium ion secondary battery: A direct Ab Initio molecular dynamics (AIMD) study, *ChemPhysChem*, 2014, **15**, 1604–1610.
- 49 E. Carrasco, M. A. Brown, M. Sterrer, H.-J. Freund, K. Kwapien, M. Sierka and J. Sauer, Thickness-dependent hydroxylation of  $\text{MgO}(001)$  thin films, *J. Phys. Chem. C*, 2010, **114**, 18207–18214.
- 50 V. Kyriakou, I. Garagounis, E. Vasileiou, A. Vourros and M. Stoukides, Progress in the electrochemical synthesis of ammonia, *Catal. Today*, 2017, **286**, 2–13.
- 51 Y. Abghoui and E. Skúlason, Onset potentials for different reaction mechanisms of nitrogen activation to ammonia on transition metal nitride electro-catalysts, *Catal. Today*, 2017, **286**, 69–77.
- 52 X. Yang, S. Kattel, J. Nash, X. Chang, J. H. Lee, Y. Yan, J. G. Chen and B. Xu, Quantification of active sites and elucidation of the reaction mechanism of the electrochemical nitrogen reduction reaction on vanadium nitride, *Angew. Chem., Int. Ed.*, 2019, **58**, 13768–13772.
- 53 X. Cui, C. Tang and Q. Zhang, A review of electrocatalytic reduction of dinitrogen to ammonia under ambient conditions, *Adv. Energy Mater.*, 2018, **8**, 1800369.
- 54 A. Seggio, F. Chevallier, M. Vaultier and F. Mongin, Lithium-mediated zincation of pyrazine, pyridazine, pyrimidine, and quinoxaline, *J. Org. Chem.*, 2007, **72**, 6602–6605.
- 55 Y. Sun, Y. Wang, H. Li, W. Zhang, X.-M. Song, D.-M. Feng, X. Sun, B. Jia, H. Mao and T. Ma, Main group metal elements for ambient-condition electrochemical nitrogen reduction, *J. Energy Chem.*, 2021, **62**, 51–70.
- 56 D. Yao, C. Tang, P. Wang, H. Cheng, H. Jin, L.-X. Ding and S.-Z. Qiao, Electrocatalytic green ammonia production beyond ambient aqueous nitrogen reduction, *Chem. Eng. Sci.*, 2022, **257**, 117735.
- 57 X. Fu, J. Zhang and Y. Kang, Electrochemical reduction of  $\text{CO}_2$  towards multi-carbon products via a two-step process, *React. Chem. Eng.*, 2021, **6**, 612–628.
- 58 K. Li, S. G. Shapel, D. Hochfilzer, J. B. Pedersen, K. Krempel, S. Z. Andersen, R. Sažinas, M. Saccoccio, S. Li, D. Chakraborty, J. Kibsgaard, P. C. K. Vesborg, J. K. Nørskov and I. Chorkendorff, Increasing current density of lithium-mediated ammonia synthesis with high surface area copper electrodes, *ACS Energy Lett.*, 2022, **7**, 36–41.
- 59 K. Li, S. Z. Andersen, M. J. Statt, M. Saccoccio, V. J. Bukas, K. Krempel, R. Sa, D. Chakraborty, J. Kibsgaard, P. C. K.



- Vesborg, J. K. Nørskov and I. Chorkendorff, Enhancement of lithium-mediated ammonia synthesis by addition of oxygen, *Science*, 2021, **374**, 1593–1597.
- 60 X. Ma, J. Li, H. Zhou and H. Sun, Continuous ammonia synthesis using Ru nanoparticles based on Li-N<sub>2</sub> battery, *Mater. Today Energy*, 2022, **29**, 101113.
- 61 A. Tsuneto, A. Kudo and T. Sakata, Efficient electrochemical reduction of N<sub>2</sub> to NH<sub>3</sub> catalyzed by lithium, *Chem. Lett.*, 1993, **22**, 851–854.
- 62 Z. Tang, X. Meng, Y. Shi and X. Guan, Lithium-based loop for ambient-pressure ammonia synthesis in a liquid alloy-salt catalytic system, *ChemSusChem*, 2021, **14**, 4697–4707.
- 63 A. Biswas, S. Kapse, B. Ghosh, R. Thapa and R. S. Dey, Lewis acid-dominated aqueous electrolyte acting as co-catalyst and overcoming N<sub>2</sub> activation issues on catalyst surface, *Proc. Natl. Acad. Sci. U. S. A.*, 2022, **119**, e2204638119.
- 64 Y. Ren, C. Yu, X. Tan, H. Huang, Q. Wei and J. Qiu, Strategies to suppress hydrogen evolution for highly selective electrocatalytic nitrogen reduction: Challenges and perspectives, *Energy Environ. Sci.*, 2021, **14**, 1176–1193.
- 65 T. Goto and Y. Ito, Electrochemical reduction of nitrogen gas in a molten chloride system, *Electrochim. Acta*, 1998, **43**, 3379–3384.
- 66 K. Kim, Y. Chen, J.-I. Han, H. C. Yoon and W. Li, Lithium-mediated ammonia synthesis from water and nitrogen: A membrane-free approach enabled by an immiscible aqueous/organic hybrid electrolyte system, *Green Chem.*, 2019, **21**, 3839–3845.
- 67 H.-L. Du, M. Chatti, R. Y. Hodgetts, P. V. Cherepanov, C. K. Nguyen, K. Matuszek, D. R. MacFarlane and A. N. Simonov, Electroreduction of nitrogen with almost 100% current-to-ammonia efficiency, *Nature*, 2022, **609**, 722–727.
- 68 N. Lazouski, K. J. Steinberg, M. L. Gala, D. Krishnamurthy, V. Viswanathan and K. Manthiram, Proton donors induce a differential transport effect for selectivity toward ammonia in lithium-mediated nitrogen reduction, *ACS Catal.*, 2022, **12**, 5197–5208.
- 69 R. Sažinas, S. Z. Andersen, K. Li, M. Saccoccio, K. Krempf, J. B. Pedersen, J. Kibsgaard, P. C. K. Vesborg, D. Chakraborty and I. Chorkendorff, Towards understanding of electrolyte degradation in lithium-mediated non-aqueous electrochemical ammonia synthesis with gas chromatography-mass spectrometry, *RSC Adv.*, 2021, **11**, 31487–31498.
- 70 L. Li, C. Tang, H. Jin, K. Davey and S.-Z. Qiao, Main-group elements boost electrochemical nitrogen fixation, *Chem*, 2021, **7**, 3232–3255.
- 71 J. M. McEnaney, S. J. Blair, A. C. Nielander, J. A. Schwalbe, D. M. Koshy, M. Cargnello and T. F. Jaramillo, Electrolyte engineering for efficient electrochemical nitrate reduction to ammonia on a titanium electrode, *ACS Sustainable Chem. Eng.*, 2020, **8**, 2672–2681.
- 72 X. Fu, J. B. Pedersen, Y. Zhou, M. Saccoccio, S. Li, R. Sažinas, K. Li, S. Z. Andersen, A. Xu, N. H. Deissler, J. B. V. Mygind, C. Wei, J. Kibsgaard, P. C. K. Vesborg, J. K. Nørskov and I. Chorkendorff, Continuous-flow electrosynthesis of ammonia by nitrogen reduction and hydrogen oxidation, *Science*, 2023, **379**, 707–712.
- 73 D. Krishnamurthy, N. Lazouski, M. L. Gala, K. Manthiram and V. Viswanathan, Closed-loop electrolyte design for lithium-mediated ammonia synthesis, *ACS Cent. Sci.*, 2021, **7**, 2073–2082.
- 74 P. V. Cherepanov, M. Krebsz, R. Y. Hodgetts, A. N. Simonov and D. R. MacFarlane, Understanding the factors determining the faradaic efficiency and rate of the lithium redox-mediated N<sub>2</sub> reduction to ammonia, *J. Phys. Chem. C*, 2021, **125**, 11402–11410.
- 75 S. J. Blair, M. Doucet, J. F. Browning, K. Stone, H. Wang, C. Halbert, J. Avilés Acosta, J. A. Zamora Zeledón, A. C. Nielander, A. Gallo and T. F. Jaramillo, Lithium-mediated electrochemical nitrogen reduction: tracking electrode-electrolyte interfaces via time-resolved neutron reflectometry, *ACS Energy Lett.*, 2022, **7**, 1939–1946.
- 76 X. Zhao, G. Hu, G. Chen, H. Zhang, S. Zhang and H. Wang, Comprehensive understanding of the thriving ambient electrochemical nitrogen reduction reaction, *Adv. Mater.*, 2021, **33**, 2007650.
- 77 H. Tao, C. Lian, H. Jiang, C. Li, H. Liu and R. Roij, Enhancing electrocatalytic N<sub>2</sub> reduction via tailoring the electric double layers, *AIChE J.*, 2021, **68**, 17549.
- 78 Q. Qin and M. Oschatz, Overcoming chemical inertness under ambient conditions: A critical view on recent developments in ammonia synthesis via electrochemical N<sub>2</sub> reduction by asking five questions, *ChemElectroChem*, 2020, **7**, 878–889.
- 79 B. Lassalle-Kaiser, S. Gul, J. Kern, V. K. Yachandra and J. Yano, In situ/operando studies of electrocatalysts using hard X-ray spectroscopy, *J. Electron Spectrosc. Relat. Phenom.*, 2017, **221**, 18–27.
- 80 Y. Yao, S. Zhu, H. Wang, H. Li and M. Shao, A spectroscopic study on the nitrogen electrochemical reduction reaction on gold and platinum surfaces, *J. Am. Chem. Soc.*, 2018, **140**, 1496–1501.
- 81 M. Nazemi and M. A. El-Sayed, Managing the nitrogen cycle via plasmonic (photo)electrocatalysis: toward circular economy, *Acc. Chem. Res.*, 2021, **54**, 4294–4304.
- 82 C. MacLaughlin, Role for standardization in electrocatalytic ammonia synthesis: A conversation with Leo Liu, Lauren Greenlee, and Douglas MacFarlane, *ACS Energy Lett.*, 2019, **4**, 1432–1436.
- 83 C. Lee and Q. Yan, Electrochemical reduction of nitrogen to ammonia: Progress, challenges and future outlook, *Curr. Opin. Electrochem.*, 2021, **29**, 100808.
- 84 C. Li, T. Wang and J. Gong, Alternative strategies toward sustainable ammonia synthesis, *Trans. Tianjin Univ.*, 2020, **26**, 67–91.
- 85 C. Guo, J. Ran, A. Vasileff and S.-Z. Qiao, Rational design of electrocatalysts and photo(electro)catalysts for nitrogen reduction to ammonia (NH<sub>3</sub>) under ambient conditions, *Energy Environ. Sci.*, 2018, **11**, 45–56.
- 86 J. Choi, B. H. R. Suryanto, D. Wang, H.-L. Du, R. Y. Hodgetts, F. M. Ferrero Vallana, D. R. MacFarlane and A. N. Simonov,



- Identification and elimination of false positives in electrochemical nitrogen reduction studies, *Nat. Commun.*, 2020, **11**, 5546.
- 87 F. Chang, W. Gao, J. Guo and P. Chen, Emerging materials and methods toward ammonia-based energy storage and conversion, *Adv. Mater.*, 2021, **33**, 2005721.

